CONGENITAL CARDIOLOGY TODAY

Timely News and Information for BC/BE Congenital/Structural Cardiologists and Surgeons

Volume 10 / Issue 1
January 2012
International Edition

IN THIS ISSUE

CONGENITAL CARDIOLOGY TODAY
Editorial and Subscription Offices
16 Cove Rd, Ste. 200
Westerly, RI 02891 USA
www.CongenitalCardiologyToday.com

UPCOMING MEDICAL MEETINGS

Evolving Concepts in the Management of Complex Congenital Heart Disease III
Jan. 19-21, 2012; San Diego, CA USA
www.rchsd.org/professionals/cme/conferencesseminars/index.htm

The 10th International Kawasaki Disease Symposium
Feb. 7, 2012; Kyoto, Japan
/www.kawasaki-disease.org/ikds2012/

12th Annual International Symposium on Congenital Heart Disease
Feb. 17-21, 2012; St. Petersburgh, FL USA
www.allkids.org/conferences

Cardiology 2012
Feb. 22-26, 2012; Orlando, FL USA
www.chop.edu/professionals/educational-resources/continuing-medical-education/cardiology-2012/home.html

Fluid-Flow Energetics for Curved or Angulated Pathways Associated with Staged Operations for the Modified Fontan Procedure

By Martin Guillot, PhD; Nancy Ross-Ascuitto MD; and Robert Ascuitto PhD, MD

Abstract

For the operations comprising the modified Fontan procedure for single-ventricle complex, blood flow is required to negotiate sharply curved or abruptly angulated (θ) passages to perfuse the lungs. We postulated such changes in flow direction would exacerbate pressure drop (ΔP), energy loss (ΔE) and shear stress, important determinates of viscous dissipation for a fluid in motion. Computational fluid dynamics (CFD) was used to model viscous fluid flowing through channels, designed to simulate blood traversing aortopulmonary or cavopulmonary Fontan connections. Viscosity values [(3-8) x 10^{-3} kg/m-s] were chosen to reflect clinically-relevant blood hematocrits (30% to 60%). Numerical solutions to the Navier-Stokes equations (finite volume analysis) were used to construct fluid pressure distributions, flow-velocity fields and contour plots of wall shear stress, along fluid pathways. The quantities ΔP(η,θ), ΔE(η,θ) and wall shear stress were found to increase significantly with rising viscosity (η) and advancing angle (θ) of flow deflection. These hemodynamic parameters were also studied for staged operations required to carry-out the modified Fontan procedure; namely, aorta-to-pulmonary artery shunt in a neonate, bidirectional Glenn shunt in a 5 month old and completed total cavopulmonary connection (TCPC) in a 36 month old. Cardiac output was assumed to be 3L/min/m^2. Simplified analytical descriptions are introduced to provide insight into fluid shear stress development and flow-energy depleting processes associated with a viscous fluid undergoing changes in pathway orientation. These findings have important clinical implications for maintaining energy efficient cavopulmonary blood flow in modified Fontan patients.

Introduction

The modified Fontan procedure is currently the surgical treatment of choice for patients with Single-Ventricle Heart Disease. The two most common forms of palliation are the atriopulmonary connection with lateral tunnel[1] and the total cavopulmonary connection (TCPC).[2-4] In the former, the systemic atrial appendage is combined with an intra-atrial baffle to direct superior and inferior vena caval blood flow to the pulmonary arteries. A shortcoming of this operation is that superior vena caval flow must bend through a large angle to reach the atriopulmonary anastomosis. In contrast, the TCPC incorporates the combination of a bidirectional Glenn shunt and a lateral extracardiac (or intracardiac) conduit from the inferior vena cava to the right pulmonary artery. The TCPC is considered to be hemodynamically superior, insomuch as it provides more laminar blood flow to the lungs. Nevertheless, abrupt and prominent changes in flow direction (90° turns) still are required to construct the cavopulmonary connections. Although both surgical approaches are designed to function without direct assistance from a ventricular pumping chamber; in doing so, the pulmonary circulation is placed in series with the systemic venous circulation, thereby producing additional afterload to systemic venous return. This arrangement creates the hemodynamic dilemma associated with Fontan

Medtronic

Hope, Restored.

A revolutionary treatment option designed to delay the need for surgical intervention.

Restore hope for your patients with RVOT conduit dysfunction.

www.Melody-TPV.com

Melody®

TRANSCATHETER PULMONARY VALVE (TPV) THERAPY

Melody® Transcatheter Pulmonary Valve

Ensemble® Transcatheter Valve Delivery System

For more information about Melody Transcatheter Pulmonary Valve Therapy, contact your Medtronic Sales Representative, your local Medtronic office or visit www.Melody-TPV.com.

Melody and Ensemble are registered trademarks of Medtronic, Inc.

The Melody Transcatheter Pulmonary Valve System and Ensemble Transcatheter Delivery System has received CE-Mark approval and is available for distribution in Europe. Additionally, a Medical Device Licence has been granted and the system is available for distribution in Canada.

anatomy: namely, "elevated systemic venous pressure yet inadequate systemic ventricular filling."

Empirical studies[2-16] and computational fluid dynamics investigations (CFD)[17-31] have shown an important factor governing successful hemodynamic performance of modified Fontan palliation is the capacity of the surgically-crafted cavopulmonary blood flow pathway to conserve the latent energy required for effective lung perfusion, (i.e. provide sufficient pulmonary blood flow for adequate oxygenation and yet enough preload for the systemic ventricle to maintain an acceptable cardiac output). Recently, using analytical models[32-34] and CFD,[35-36] we found significant energy losses arise when passive flow is required to traverse even modest anatomical obstruction (abrupt increase or decrease in vessel cross-sectional area) and/or to overcome relevant functional obstruction (high fluid viscosity). Energy dissipation, however, may also occur when flow is required to negotiate an acute bend in its pathway, as with Glenn shunts. Sudden changes in vessel or conduit direction can unfavorably alter fluid-pressure distributions, distort flow-velocity profiles and increase fluid shear stresses, so as to worsen flow-energy expenditure. In each case, the fluid's viscosity becomes an important factor in determining the degree of energy wastage. Therefore, the purpose of this investigation is two-fold:

1. To help conceptualize energy-depleting blood flow processes relevant to modified Fontan anatomy and
2. To update clinicians on the use of CFD to design more energy-sparing cavopulmonary blood flow passages.

Insomuch as a single ventricle must support the entire cardiovascular circulation, it is generally believed an understanding of interrelationships between "Fontan cavopulmonary morphology and economy of blood flow energy utilization" can have important implications for improving long-term clinical outcome in these patients.

Materials and Methods

Model Description

Non-pulsatile, incompressible, viscous-fluid flowing through a vessel or conduit was taken to satisfy the steady-state mechanical-energy balance equations:

$$\Delta P = (\langle P \rangle_i - \langle P \rangle_f) \quad (1a)$$
$$\Delta P = (\langle K \rangle_f - \langle K \rangle_i) + \Delta E. \quad (1b)$$

The terms <P> and <K> represent "flow-averaged" pressure (P) and "flow-averaged" kinetic energy (K), respectively. The quantity ΔE denotes flow-energy loss associated with dissipative processes. The subscripts (i) and (f) designate the initial (i) position for unperturbed (incoming) and the final (f) position for equilibrating (outgoing), fluid flow. The various terms, and the flow-averaging procedures, are defined in Appendix A. Equations (1) describe the overall change in pressure (ΔP) and kinetic energy (ΔK), and the flow-energy loss (ΔE), associated with the fluid transition (i →f). The quantities ΔP, ΔK and ΔE depend on viscosity and flow rate, along with anatomical features of the fluid pathway. The terms ΔK and ΔE represent energy per unit of fluid volume and are usually expressed as (Joules/m^3). However, since they are part of Equation (1), along with ΔP, we chose to express ΔK and ΔE in equivalent units of (Newtons/m^2). Numerical solutions to the fluid-flow (Navier - Stokes) equations were used to construct fluid-pressure distributions, flow-velocity fields and flow-velocity gradients from which ΔP, ΔK, ΔE and fluid shear stress at the vessel wall – i.e., *wall shear stress* – were determined. For the fluid pathways considered, we identified regions of

high shear stress (platelet activation and viscous dissipation) and low shear stress (fluid stasis and thrombus formation). The fluid was assumed to be of Newtonian character, a generally valid approximation to study blood flow behavior through larger vessels.

Model Parameters

I. Fluid Pathways with Angulation or Bifurcation

Flow energetics - pressure drop, energy loss and fluid shear stress - was studied for a viscous fluid traversing an angulating or bifurcating pathway. For an angulated vessel (Figure 1A), deflections (θ) were taken as 0º, 30º, 60º and 90º - unilateral Glenn shunt. For a bifurcated vessel (Figure 1B), the angle was taken as 90º, forming a "T" pathway - bidirectional Glenn shunt. Viscosity values (η) for the calculations were based on data collected from in-vitro experiments relating viscosity to hematocrit for whole blood[37]. Based on the findings of Wells and Merrill[38], we used viscosity values ranging from (3 – 8) X 10^{-3} kg/m-s, corresponding to hematocrits of (30% - 60%). (The viscosity of plasma (37ºC) is ~ 1.8 X 10^{-3} kg/m-s.). For simplicity, relative viscosity (i.e. relative to the viscosity of water, 1 X 10^{-3} kg/m-s) - was used in discussions or to label figures. Fluid density was 1060 kg/m^3. The initial fluid pathways studied were taken to have an overall length of 0.1 m and a diameter (D) of 0.012 m. A flow rate of 1.67 X 10^{-5} m^3/s (1.0 L/min)

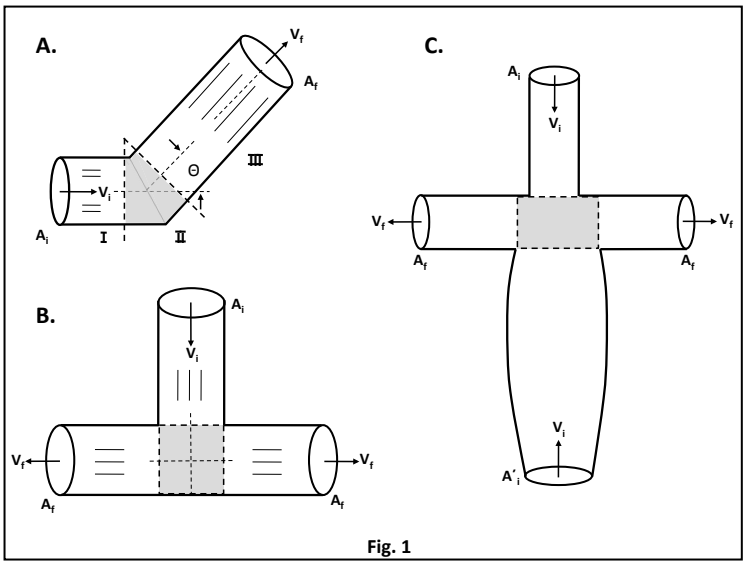

Figure 1. Schematic representation of the tubular fluid pathways considered. [A]. The angulated (θ) pathway. This pathway was considered to be composed of three sections, I, II and III (see Appendix B). Sections I and III are taken as resistance vessels. Section II represents the narrow region where flow undergoes the sudden change in direction through an angle (θ). [B]. The bifurcated (90º) pathway – bidirectional Glenn shunt. [C]. The totalcavopulmonary connection (TCPC) without offset of the inferior vena cava to right pulmonary artery conduit. Here A_i (A_f) represent the incoming (outgoing) vessel cross-sectional areas, and V_i (V_f) the corresponding flow velocities. Shaded areas represent primary regions of fluid mixing.

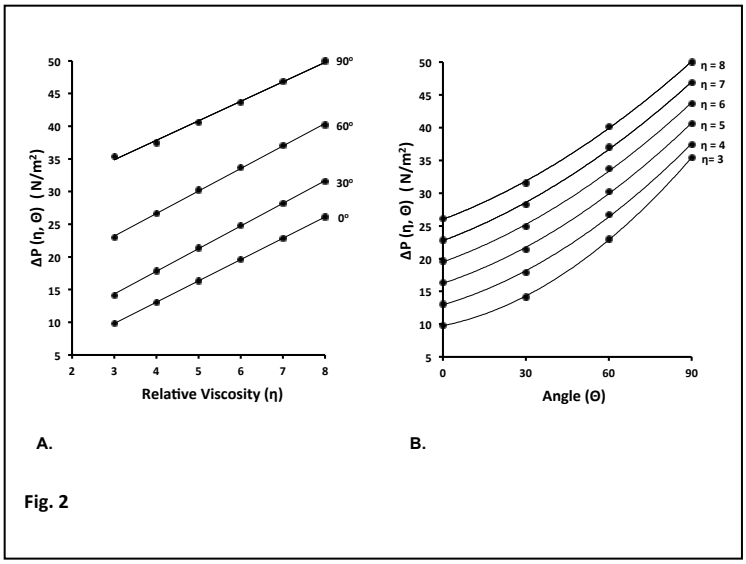

Fig. 2

Figure 2 [A]. Shows pressure drop ΔP(η,θ), in N/m², on the y-axis and relative viscosity (η), unitless, on the x-axis, for each angle (θ) of deflection, in degrees. [B]. Shows pressure drop ΔP(η,θ), in N/m², on the y-axis and angle (θ) of deflection, in degrees, on the x-axis, for each value of relative viscosity (η).

was used for these calculations. The pressure drop, ΔP (η,θ), and flow-energy loss, ΔE (η,θ), were plotted against relative viscosity and angle of flow deflection. Likewise, contour plots of wall shear stress, an important determinant of flow-energy dissipation, are shown for representative values of relative viscosity, namely 3, 5 and/or 8.

II. Fluid Pathways Associated with Stages of the Modified Fontan Procedure (TCPC)

Flow dynamics was studied for a viscous fluid, chosen to represent blood flowing through pathways associated with staged operations comprising the modified Fontan procedure. Three age-appropriate fluid pathways were computationally constructed to simulate a:

- central aorta to pulmonary artery shunt,
- bidirectional Glenn shunt and
- total cavopulmonary connection.

1. A tubular vessel was used to describe a typical central aorta to pulmonary artery shunt required to provide pulmonary blood flow in a neonate. The diameter of the vessel was selected as 0.004 m. The course taken by the vessel was deduced from a representative CT angiogram in a patient, whose shunt thrombosed. The mean proximal (inflow) pressure was set at 7292 N/m² (55 mmHg) and the distal (outflow) pressure at 1989 N/m² (15 mmHg). In this case, rather than a prior fixing the magnitude of the flow, flow rate was determined by the overall pressure drop 5303 N/m² (40 mmHg) along the vessel.
2. Tubular vessels were combined to form a "T" pathway, to represent a bidirectional Glenn shunt (Stage II of the modified Fontan procedure) (Figure 1B). It was assumed the Glenn shunt would be placed in a patient at about 5 months of age. At the 50th percentile, patient weight is 7.2 kg and BSA 0.35 m². The right pulmonary artery (RPA), left pulmonary artery (LPA) and superior vena cava (SVC) are 0.006 m in diameter (Z score of zero). Cardiac output was taken as 3L/min/m². The corresponding SVC flow rate was approximated as ~ 0.7L/min (or ~ 2L/min/m²).
3. Tubular vessels were joined to form a "Cross" pathway, to represent a completed total cavopulmonary connection (Stage III of the modified Fontan procedure) (Figure 1C). It was assumed modified Fontan completion would take place in a patient at about 36 months of age. At the 50th percentile, patient weight is 14.4 kg and BSA 0.6 m². The RPA, LPA and SVC are 0.009 m in diameter (Z score of zero). The inferior vena cava (IVC) was taken as 0.012 m in diameter[39]. The IVC to RPA distance was considered to be 0.040 m[39]. The mid-conduit diameter was selected as 1.5 times the diameter of the IVC, or 0.018 m[40]. It has been suggested 0 .018 m conduits are optimal for children ~ 3 years old[41]. Again, cardiac output was selected as 3L/min/m². The IVC flow was assumed to be 1.5 times that of the SVC; thus, IVC flow is 1.1L/min (or ~ 1.8L/min/m²) and SVC flow is 0.7L/min (or ~ 1.2L/min/m²).

Numerical Analysis

Flow simulation studies were performed using the commercial CFD package - Fluent 12.1 (Ansys, Inc., Lebanon, NH)

Fluent is a general purpose CFD software program capable of numerically solving the Navier-Stokes equations using finite volume analysis. In this study, we computed steady state solutions to the 3-dimensional fluid-flow equations, for geometries relevant to operations comprising stages of the Fontan procedure. Although blood can display non-Newtonian behavior, this study was limited to Newtonian models. The large diameter vessels and the range of shear rates encountered justify use of this approximation.

Mesh Generation

Finite volume analysis was employed to numerically solve the Navier-Stokes equations. The procedure involves dividing the computational domain into a number of contiguous volume elements, called cells. Meshes, which are a collection of finite volumes, were constructed over the 3-dimensional computational domain and were generated using the ICEM-CFD software program (Ansys, Inc, Lebanon, NH). "Coarse" and "fine" meshes were utilized for each of the cases studied. The number of volumes for the fine meshes ranged from 1.5 - 2.0 million cells, depending on the particular fluid pathway considered. The CFD analysis was performed with both coarse and fine meshes, to ensure numerical solutions were independent of mesh size. Some of the pathways exhibited geometric symmetry. For example, the angulation cases are symmetric about a center plane. Whenever possible, such symmetry was exploited to simplify numerical computations. The 3-D meshes were constructed from hexahedral volumes into an unstructured mesh. Prismatic elements were generated for domains near vessel walls to increase computational accuracy. This method is crucial when computing quantities such as wall shear stress, which is highly dependent on velocity gradients.

Boundary Conditions

Solutions to the Navier-Stokes equations require imposing boundary conditions on the computational domain. For the geometries of the fluid pathways considered, boundary conditions are required at the: flow inlet,

vessel wall and flow outlet. The Reynolds number for inlet flow, $Re_D = \rho V_{avg} D/\eta$, ranged from 300 to 600, consistent with essentially laminar flow. The incoming fluid stream exhibited fully developed flow (parabolic velocity profiles) prior to encountering the change in vessel direction. The parabolic velocity profiles specified at the inlet were such that V_{avg} multiplied by the cross-sectional area of the vessel yielded the desired flow rate. The "no-slip" boundary condition (zero velocity) was imposed at the vessel wall. The downstream pressure at the flow outlet was fixed at 1591 N/m^2 (12 mmHg), typical of Fontan-like pulmonary artery pressure. As a comparison, we also performed flow analysis for a "T" pathway in which the left branch is diffusely narrowed (half the diameter of the right branch). In this case, the right branch outlet pressure was retained as 1591 N/m^2 (12mmHg), whereas the left branch outlet pressure was reduced to 1326 N/m^2 (10mmHg).

Results

I. Fluid Pathways with Angulation or Bifurcation

For the angulated fluid pathway (Figure 1A), flow-averaged pressure drop, $\Delta P(\eta,\theta)$, increased uniformly with respect to increasing viscosity (η) (Figure 2A), and angles (θ) of deflection (Figure 2B). The rate of rise or slope of the regression line relating $\Delta P(\eta,\theta)$ to η was similar for each angle (30^o, 60^o and 90^o – the unidirectional Glenn shunt), averaging 3.3 N/m^2. Likewise, $\Delta P(\eta,\theta)$ increased with advancing angle (θ), although there was a small quadratic component ($\sim 0.001\theta^2$) contributing to the nearly linear regression line, for each value of η. As with $\Delta P(\eta,\theta)$, the flow-averaged flow-energy loss, $\Delta E(\eta,\theta)$, increased progressively with respect to increasing viscosity (η) (Figure 3A), and angles (θ) of deflection (Figure 3B). The slope of the regression line relating $\Delta E(\eta,\theta)$ to η was similar for each angle (θ), averaging 2.9 N/m^2. The $\Delta E(\eta,\theta)$ increased linearly with advancing angle (θ), for each value of η. The slopes of the lines relating $\Delta E(\eta,\theta)$ to θ, were nearly identical, averaging 0.3N/m^2. For the bifurcated (90^o) pathway (Figure 1B), $\Delta P(\eta,90^o)$ and $\Delta E(\eta,90^o)$ also increased linearly with respect to rising viscosity (η). However, the slope of the regression line relating $\Delta E(\eta,90^o)$ to η was considerably less for the bidirectional Glenn shunt (1.1 N/m^2), compared to the unidirectional Glenn shunt (2.7 N/m^2).

For a representative angulated (60^o) pathway, contour plots of wall shear stress are displayed in Figure 4, for relative viscosity values of, 3, 5 and 8. For the incoming fluid stream, shear stress is low (< 0.5 N/m^2). However, beyond the angulation, there is a localized region (red/yellow) of high wall shear stress (2.5 – 3.5 N/m^2), created as the incoming horizontally moving fluid stream impacts the opposing vessel wall. Moreover, elevated shear stress (~ 2 N/m^2) persists (resolves slowly) along the downstream portion of the pathway, increasing in extent with increasing viscosity. For the bifurcated (90^o) pathway, wall shear stress (2.5 – 4.5 N/m^2) becomes symmetrically-distributed opposite the incoming vessel, and extends further into the branches as viscosity increases. This pattern of wall shear stress is discussed in more detail below, in the context of a bifurcated pathway (bidirectional Glenn shunt) associated with Stage II of the modified Fontan procedure.

II. Fluid Pathways Associated with Stages of the Modified Fontan Procedure (TCPC)

For a simulated aorta to pulmonary artery shunt in a neonate, a contour plot of wall shear stress is shown in Figure 5. At the vertex of the tubular vessel, where flow curvature is sharpest, shear stress increases 5-8 fold, or (150 – 220 N/m^2), (orange/green), for relative viscosity values of 3, 5 and 8, corresponding to hematocrits of 30% - 60%. Likewise, near the outlet of the vessel, there is a second section of lesser curvature oriented in the opposite direction. Here as well, shear stress is elevated (green), reaching its greatest value at the point of maximum curvature.

For a simulated bidirectional Glenn shunt placed in a 5 month old (Stage II of the modified Fontan procedure), corresponding contour plots of wall shear stress are shown in Figure 6, for relative viscosity values of 3, 5 and 8. As can be seen, again there is a symmetrically-distributed region of elevated shear stress (25 – 35 N/m^2) opposite the incoming vessel (SVC) of the bifuricated (90^o) pathway. In the distal branches of the "T", shear stress falls to considerably lower values, (< 3N/m^2), as outgoing flow re-equilibrates. For comparison, Figure 7 shows plots of wall shear stress for a bidirectional Glenn shunt in a 36 month old, but with the left branch half the diameter of the right branch, for relative viscosity values of 3, 5 and 8. Now, the region of elevated wall shear stress becomes unequally distributed with respect to the incoming vessel (SVC), and is biased toward the smaller left branch of the pathway. Moreover, in addition to shear stress being high juxtaposed to the incoming vessel, its greatest value (9 N/m^2) is reached at the origin of the narrowed left branch, and continues elevated (~5N/m^2) throughout the remaining portion of the vessel.

For a simulated completed TCPC in a 36 month old (Stage III of the modified Fontan procedure), Figure 8 shows contour plots of wall shear stress, for representative relative viscosity values of 5 and 8. Symmetry planes were not employed for these calculations. The full 3-D flow fields were used to assess fluid mixing in the region defined by the junction between the incoming and outgoing vessels The incoming vessels (SVC and IVC to RPA conduit) exhibit minimal shear stress (blue), reflecting the low flow velocity near the walls of these channels. However, at the junction of the incoming vessels and outgoing branches, there are symmetrically-distributed areas (red/yellow) of high shear stress. These regions of elevated shear stress protrude progressively into the branches, as viscosity increases. Figure 9 maps the corresponding flow-velocity distributions, over intersecting planes within the vessels. For the incoming vessels, velocity near the center line is greatest consistent with the laminar nature of the flow. However, within the outgoing branches, high velocity streams (red/orange flames) emerge. Conversely, pockets of exceedingly low velocity can be identified within the proximal portions of the branches (see internal arrow).

Disussion

Fontan and Baudet[42] reported performing the first operation to fully bypass the right heart in 1971. The right atrium was included in the cavopulmonary pathway, as a pump to facilitate flow of blood to the lungs. However, many of these patients subsequently developed low cardiac output, systemic arterial oxygen desaturation, progressive right atrial enlargement and atrial rhythm disturbances. Various modifications of the Fontan operation followed in an attempt to improve hemodynamic efficiency. However, in the mid-1980s, a breakthrough occurred when deLeval and colleagues[4] empirically demonstrated that a large valveless chamber (even a pulsatile one) interposed in a fluid pathway impairs forward flow, by creating retrograde and swirling flow patterns, thereby exacerbating flow-energy losses. Thus, to this end, deLeval et al.[4], Puga et al.[43] and Pearl et al.[44] devised the TCPC, or modified Fontan procedure, the combination of a bidirectional Glenn shunt followed by a conduit connecting the inferior vena cava to the right pulmonary artery. It was reasoned direct caval pathways to the pulmonary arteries (rather than requiring systemic venous return to pass through the right atrium) would result in more streamline (energy-sparing) blood flow behavior. Nevertheless, the associated cavopulmonary connections still require blood-flow to undergo acute deflections through large angles in order to reach the lungs. In general, any curved or angulated fluid passage offers some resistance to the required change in flow direction. As such, additional pressure head and energy expenditure are needed, beyond those required to overcome dissipative forces associated with an otherwise equivalent straight line pathway.

An important part of this study is to show pressure drops and flow-energy losses increase significantly, both with increasing viscosity and advancing angles of defection (Figures 2 and 3). Insomuch as the final (downstream) pressure is held fixed at 1591 N/m^2 (12mmHg), the increase in $\Delta P(\eta,\theta)$ with increasing viscosity reflects the greater pressure head required to maintain the desired flow rate of $1.67X10^{-5}$m^3/s (1 L/min). The linearity of the relationships between fluid-pressure drop,

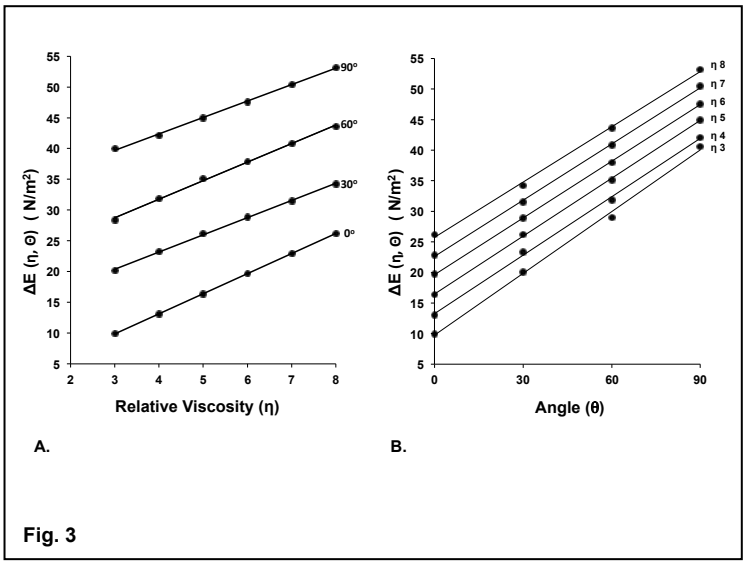

Fig. 3

Figure 3 [A]. Shows flow-energy loss ΔE(η,θ), in N/m², on the y-axis and relative viscosity (η), unitless, on the x-axis, for each angle (θ) of deflection, in degrees. [B]. Shows flow-energy loss ΔE(η,θ), in N/m², on the y-axis and angle (θ) of deflection, in degrees, on the x-axis, for each value of relative viscosity (η).

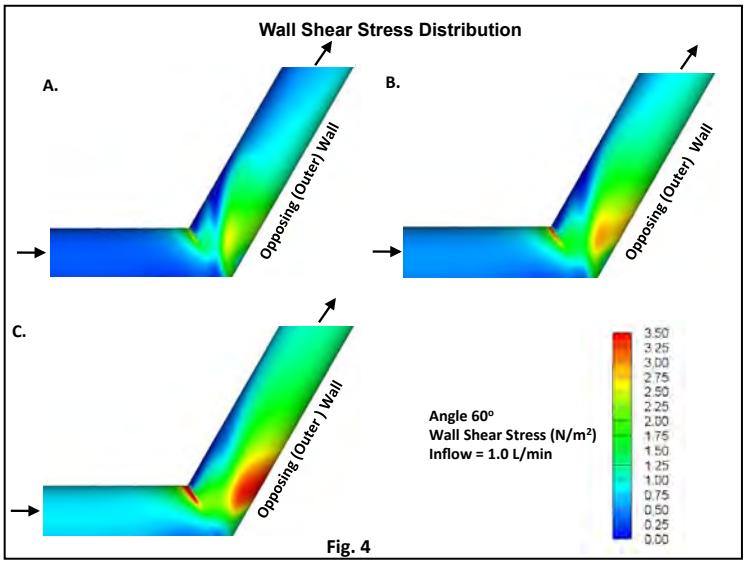

Fig. 4

Figure 4. Contour plots of wall shear stress, in N/m², for the angulated (60°) fluid pathway. Incoming flow rate is 1.0 L/min. Representative relative viscosity (η) values are: A. η = 3, B. η = 5 and C. η =8.

flow-energy loss and viscosity, and the magnitudes of the slopes of the regression lines relating these quantities, can be understood by utilizing a simplified model of passive (Poiseuille) flow through angulated tubular resistance vessels (see Appendix B, and refs.[32, 35-36] In this model, viscous and inertial effects, although individually important, are assumed to be weakly coupled. Thus, ΔE(η,θ) can sensibly be partitioned as follows, ΔE(η,θ) = [ΔE(η) +ΔE(θ)], where ΔE(η) represents the viscous (depending only on η) and ΔE(θ) the inertial (depending on θ) components of the flow-energy loss.

The primarily viscous component of ΔE(η,θ), namely ΔE (η) is taken as $(8\pi\ L/A^2)\eta Q$, which describes functional resistance to flow; L is length and A cross-sectional area of the vessel. Thus, as with computational fluid dynamics (CFD), this model predicts ΔE(η,θ) to vary directly with

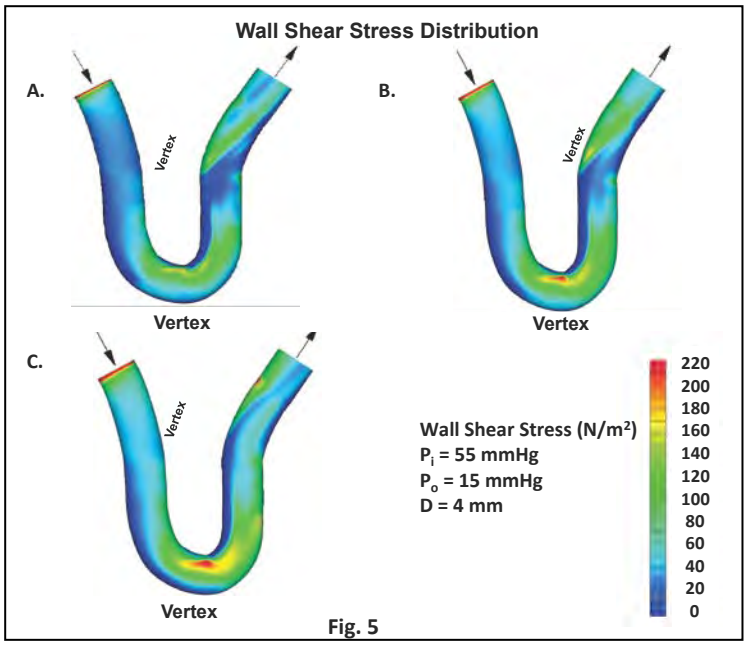

Fig. 5

Figure 5. Contour plots of wall shear stress, in N/m², for the tubular (D = 4 mm) fluid pathway – central aorta to pulmonary artery shunt. Flow rate is determined by the overall pressure drop (40 mmHg). The incoming mean pressure (P_i) is 55 mmHg and the outgoing mean pressure (P_0) is 15 mmHg. Representative relative viscosity (η) values are: A. η = 3, B. η = 5, and C. η = 8. Vertex is the site of the vessel where curvature is greatest (smallest radius of curvature).

respect to η, flow rate being held fixed (Figure 3A). Moreover, the slope of each regression line relating ΔE(η,θ) to η is 3.2 N/m², compared to an average value of 2.9 N/m² obtained from the CFD calculations. The primarily inertial component of ΔE(η,θ), namely $\Delta E(\theta) = \rho/A^2\ (1-\cos\theta)Q^2$, accounts for energy loss associated with the abrupt change in velocity of the fluid stream, as a consequence of flow bending through the angle θ; ρ is fluid density (Figure 3B). In the range 30° to 90°, the function (1- cos θ) is relatively linear; thus, the slope of the lines relating ΔE(η,θ) to θ, defined here as [{ΔE(90°) - ΔE(30°) }/60°], is 0.33 N/m², compared to an average of 0.32 N/m² obtained from the CFD calculations. Considering the simplicity of this model, the agreement with CFD calculations is quite good. However, flow derangements, such as non-laminar propagation and distribution of shear stress, cannot be ascertained without numerically solving the fluid dynamics equations.

Pressure drops and flow-energy losses for the bifurcated fluid pathway were also found to increase linearly with increasing viscosity. Importantly, the CFD calculations predict both pressure drop and flow-energy loss for the bifurcated (90°) pathway- bidirectional Glenn shunt - to be only ~ 70% of corresponding values for the angulated (90°) pathway – unidirectional Glenn shunt. Although in both cases the incoming and net outgoing flow rates are equal in magnitude, with the bifurcated fluid pathway, outgoing flow is distributed over twice the vessel cross-sectional area. One can understand the improved energy efficiency of the bidirectional Glenn shunt by considering its branches to act as resistance vessels connected in parallel (see below*). Computational fluid dynamics provides an average value of ΔE, for the various viscosity values considered, to be ~ 33 N/m²; the simplified analytical model introduced above yields 29-35 N/m², depending on how one chooses to describe flow's velocity change in Section II of the pathway (Figure 1).

** Flow through the angulated (90°) pathway – unidirectional Glenn shunt – may be compared to a direct electrical current (I) passing through two resistors, (R_1) and (R_2), connected in series; (R_1) for the incoming and*

(R_2) the orthogonal outgoing vessel. The power dissipated is ($R_1 + R_2$) I^2. In contrast, the bifurcated (90°) pathway – bidirectional Glenn shunt – is analogous to the direct current (I) passing through resistor (R_1), but then dividing to flow through two resistors, each (R_2), connected in parallel. Now, the power dissipated is ($R_1 + R_2/2$) I^2. The ratio of the powers dissipated in the two circuits is [($R_1 + R_2/2$)/($R_1 + R_2$)]. For our fluid problem, R is directly proportional to the length (L) of the vessel segment. Thus, insomuch as the cross-sectional areas of the vessels are equal, the ratio of the power losses would be [($L_1 + L_2/2$)/($L_1 + L_2$)], incoming flow rate being fixed. The length L_1 = 0.03m and L_2 = 0.07m, which predicts energy loss for the bifurcated (90°) pathway to be ~65% of that for the angulated (90°) fluid pathway, in good agreement with CFD.

A clinically relevant finding from our CFD study is that for a passively perfused fluid system, taken to simulate blood flowing through portions of a modified Fontan cavopulmonary pathway, abrupt curvature or angulation can result in marked distortion of the flow-velocity profile, unfavorable increases in fluid wall shear stress and angle-dependent viscous dissipation of energy. These effects can illicit relatively small pressure drops. With modified Fontan anatomy, such modest pressure changes largely reflect the low velocity of systemic venous flow, rather than implying insignificant energy depleting flow perturbations[35-36]. In general, pressure drop (ΔP) is determined by the change in flow kinetic energy (ΔK) plus the associated flow-energy loss (ΔE), for a fluid transition (i → f), i.e. $\Delta P = \Delta K + \Delta E$, where $\Delta K = K_f - K_i$.

In the case of an angulated (θ) fluid pathway, insomuch as there is no significant alteration in the cross-sectional area, continuity of flow requires the overall change in kinetic energy to be small ($K_f \sim K_i$). Thus, pressure drop ΔP arises primarily as a consequence of flow's dissipative energy loss. Alternatively stated, the overall fluid energy loss manifests itself primarily through the pressure drop ΔP for the fluid reaction. This result simply follows from energy balance, i.e. work performed by pressure force is needed to overcome the energy loss associated with a viscous fluid in motion. In contrast, for the bifurcated (90°) pathway, with branches of equal cross-sectional area, $K_f \sim K_i/2$ and $\Delta P \sim -K_i/2 + \Delta E$; indicating pressure drop for a fluid transition can be smaller in magnitude than the corresponding flow-energy loss. This result cautions the practitioner that, during cardiac catheterization, small pressure changes measured in a cavopulmonary pathway of a bidirectional Glenn shunt may not be indicative of the severity of the underlying flow-energy wastage; and, again emphasizes the importance of assessing vessel sizes and shapes using complementary imaging studies.

When viscous fluid flows along a stationary vessel wall, friction between the wall and the moving peripheral fluid stream sets up a retarding (drag) force, thereby generating shear stress along the vessel wall – the so-called "wall shear stress." This stress varies as ($\sim \eta Q/D^3$). Moreover, if the vessel undergoes an acute change in orientation and/or contains a sharp bend in its course, it interrupts the inertial path of the incoming fluid stream. Flow's altered direction imparts momentum to the opposing vessel wall, thereby increasing pressure on the bounding surface. Such a local change in distending pressure augments wall shear stress. (The situation is analogous to kinetic friction slowing an object as it slides along a rough surface. The frictional force opposing the motion is proportional to the object's normal force or load acting on the surface, i.e. the larger the normal force, the greater the magnitude of the retarding frictional force.) Insomuch as shear stress directly reflects fluid viscosity and flow velocity gradients, i.e. ($\sim \eta dv/dr$), it becomes an important determinate of irreversible flow-energy loss when hematocrit is high and/or there are sudden changes in fluid speed and direction. Thus, for these reasons, we assessed wall shear stress along the blood flow pathways considered in this study.

For the angulated (θ) fluid pathway (Figure 1A), flow advancing beyond the angulation junction impacts the opposing vessel wall, along a distance of ~ D/(2 tan θ) (Figure 4). The incoming flow's momentum ($\rho Q_i V_i$) can be decomposed into two parts. One part ($\rho Q_i V_i \cos \theta$) runs parallel to the central axis of the angulated vessel and contributes to the driving force for outgoing flow. The complementary portion ($\rho Q_i V_i \sin \theta$) acts perpendicular to the central axis and biases advancing flow toward the outer wall of the vessel (Figure 4). This component of the flow's momentum gives rise to a "velocity and angle"-dependent increase in wall shear stress beyond the junction (depicted by the red, yellow and downstream green regions).

With a bifurcated (90°) pathway (Figure 1B), the branches generally have a combined cross-sectional area greater than that of the incoming vessel. This situation leads to a decrease in flow velocity and a corresponding reduction in the net outgoing flow-kinetic energy. Thus, excess kinetic energy that entered the region of bifurcation must be dissipated. Some of this energy is converted into pressure (via the Bernoulli effect), while the remainder is degraded through frictional forces. Insomuch as there is equal division of flow into the branches, the local increase in pressure gives rise to a symmetrically distributed region of high wall shear stress (as indicated by the red, yellow and green areas in Figure 6). With modified Fontan anatomy and passive cavopulmonary blood flow, the retarding nature of high shear stress can predispose to sluggish flow, and thereby provide conditions for thrombus formation.

Another part of this investigation was to employ CFD to assess flow characteristics that may impair effective perfusion through surgically-constructed aortopulmonary or cavopulmonary connections required to carry out stages of the modified Fontan procedure. For the simulated central aorta to pulmonary artery shunt, our findings suggest, for the sizes (~ 4mm) of the tubular grafts required to provide blood flow to the lungs in a neonate, the degree of curvature in the vessel can have a profound impact on maintaining patency of the shunts. As shown in Figure 5, fluid shear stress increases dramatically as flow traverses bends in the simulated central shunt. The importance of vessel curvature on shear stress development can be understood by considering its relationship to other important flow parameters. The magnitude of wall-shear stress depends directly on fluid viscosity (η), inversely on the cube of the vessel's radius of curvature (R) and linearly on flow rate (Q), i.e. ~ (η/R^3)Q. Thus, the higher the fluid viscosity and the smaller the radius of curvature (sharper the bend in the vessel), the greater the shear stress generated within the angulating fluid, where centrifugal effects already are important. As flow executes a sharp turn in a vessel, its velocity profile becomes skewed, moving away from the center of curvature. The layer of fluid with the highest velocity moves from the centerline radially outward towards the vessel wall. In this way, a greater distending pressure is created at curved portions of the vessel, thereby increasing wall shear stress in these regions.*

** If one considers fluid moving along a streamline for curved flow, pressure increases by an amount $\rho V^2/R$, per unit of distance outward along the radius of curvature, where V is the speed and R the radius of curvature. Moreover, the product VR is essentially constant. Thus, the fluid's speed will be greater near the inner compared to the outer wall of the vessel. Conversely, by the Bernoulli effect, the corresponding pressure becomes larger near the outer compared to the inner wall.*

Shunt size, vessel curvature and high fluid shear stress (or shear rate) can have important implications for shunt failure. A common cause of shunt occlusion in neonatal patients is thrombus formation within the graft. Although Gore-Tex itself is likely not pro-atherogenic, we find wall shear stresses (150 - 220 N/m^2) and shear rates (30,000 - 44,000/s) at sites of shunt curvature, easily high enough to induce platelet activation in-vivo.[45,46] It has been well established that platelet aggregation and activation from shear stress interactions can initiate and sustain the blood clotting cascade. Thus, it appears disordered blood flow in conjunction with pathologically high values of shear stress at regions of sharp curvature can contribute to stenosis and thrombus formation within a shunt, especially in the small-diameter grafts required in a neonate.

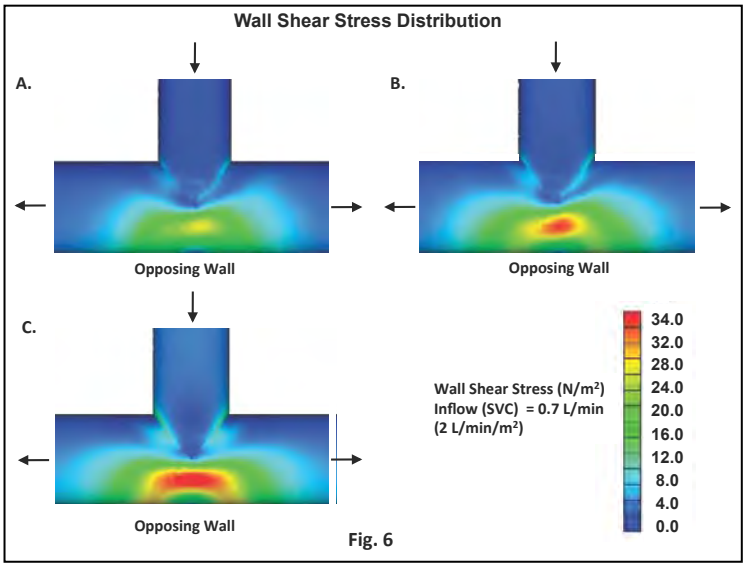

Figure 6. Contour plots of wall shear stress, in N/m², for the bifurcated (90°) fluid pathway – bidirectional Glenn shunt (Stage II of the modified Fontan procedure). Incoming (SVC) flow rate is 0.7 L/min (or 2L/min/m²). Representative relative viscosity (η) values are: A. η = 3, B. η = 5, and C. η = 8. Note, wall shear stress is symmetrically distributed, with respect to the axis of the incoming vessel (SVC). Incoming (SVC) = outgoing (R-branch) = outgoing (L-branch) = 0.006m in diameter.

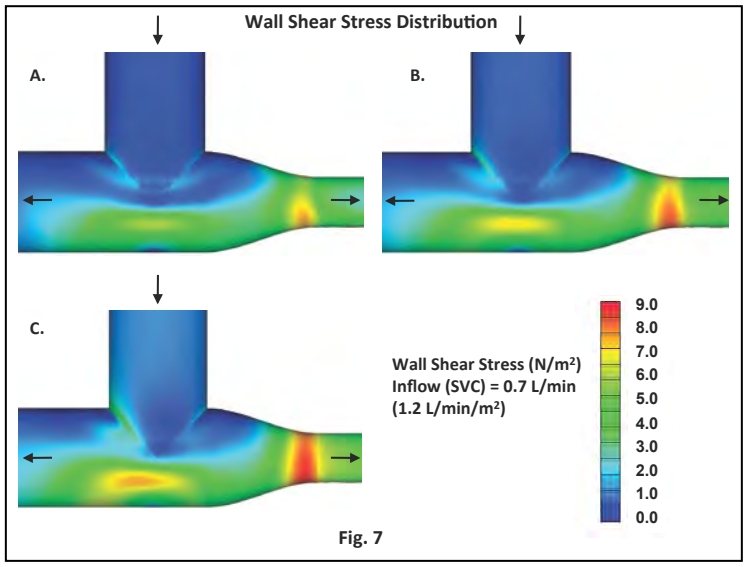

Figure 7. Contour plots of wall shear stress, in N/m², for the bifurcated (90°) fluid pathway – bidirectional Glenn shunt (just prior to competing a modified Fontan procedure or TCPC). Incoming (SVC) flow is 0.7L/min (or 1.2 L/min/m²). Relative viscosity (η) are: A. η = 3, B. η = 5, and C. η = 8. In this case, the left branch is diffusely narrow (half the diameter of the night branch). Note, wall shear stress is asymmetrically distributed with respect to the axis of the incoming vessel (SVC), (compare with Figure 6). Incoming (SVC) = outgoing (R-branch) = 0.009 m in diameter. Outgoing (L-branch) = 0.0045 m in diameter.

For a simulated birdirectional Glenn shunt placed at 5 months of age (Stage II of the modified Fontan procedure), we found high wall shear stress opposite the incoming vessel (SVC), as shown in Figure 6. The greater magnitude of shear stress associated with the bidirectional Glenn shunt perfusing 0.006 m branches (~ 30 N/m²), compared to that obtained with the 0.012 m branches considered earlier (~ 3.5 N/m²), reflects wall shear stress's inverse dependence on the cube of the vessel diameter (~ 1/D³). Figure 7 illustrates important rearrangement of shear stress arising when one of the branches of a bidirectional Glenn shunt is stenotic, a not uncommon clinical situation. Now, wall shear stress maps differently in the two branches, as a consequence of the unequal vessel diameters and flow rates. The higher wall shear stress in the narrowed left branch leads to an entrance energy loss (circumferential red area), in addition to increased viscous dissipation throughout the contiguous reach (green region). These findings again signal the importance of addressing focal and/or diffuse stenoses in branch pulmonary arteries prior to completing the modified Fontan procedure.

For a simulated TCPC in a 36 month old (Stage III of the modified Fontan procedure), CFD predicts high wall shear stress (red areas) protruding into the outgoing vessels, as shown in Figure 8. This pattern emerges as a consequence of the incoming fluid streams (SVC and IVC to RPA conduit) colliding, and thereby dispersing disturbed flow laterally into the branches. Figure 9 shows corresponding flow-velocity contours as distributed over intersecting planes within the vessels. Of clinical importance are the regions (dark blue) of exceedingly low flow velocity (< 0.04 m/s) along the medial and lateral aspects of the IVC to RPA conduit. Likewise, isolated pockets of low velocity are identified in the proximal outgoing branches (pulmonary arteries). Such areas of flow stagnation along the walls of the conduit are potentially high-risk for thrombus formation, being especially relevant in the presence of a fenestration.[41] Of course, the actual nature of these low velocity flow disturbances arising in a TCPC will depend on the size, shape and course (extra-vs intra-cardiac) of the IVC to RPA conduit. In the case of an extra-cardiac IVC to RPA connection, for example, the flow's lowest velocity stream is displaced laterally along the outer wall of the conduit, rather than bilaterally as in Figure 9, because of the concave nature of the surgically constructed passage. Moreover, the distribution and morphology of pulmonary vessels beyond the proximal branches (LPA and RPA), i.e. downstream from the Fontan junction, may be required to realistically assess cavopulmonary flow energetics for the in-vivo situation. In a sense, specifics of Fontan patients' cavopulmonary anatomy may be required, in order to formulate management plans and design interventional and surgical procedures to help optimize pulmonary blood flow energy utilization.Collaborative efforts among research teams may be needed to develop new hemodynamic strategies for the treatment of these complex patients.

After nearly 40 years of Fontan experience and unmitigated surgical success in diverting blood flow from the vena cave to the lungs without assistance of a right ventricular pumping chamber, the Fontan procedure's glaring residual and unrelenting hemodynamic deficiencies – elevated systemic venous pressure and non-pulsatile cavopulmonary blood flow – have been painfully apparent from their associated clinical sequelae - hepatic cirrhoses, blood coagulopathies, thrombus formation, protein-losing enteropathy, pulmonary arteriovenous fistulae, low cardiac output and systemic ventricular contractile dysfunction. Research based on cogent empirical methods and cherished elements of fluid dynamics has helped design more energy – efficient blood flow passages. Various modeling studies have focused on effects of: atriocavopulmonary pathway morphology,[2,12,15,32-33,35-36] energy-depleting blood flow disturbances,[2,21,23,35,36,41] colliding caval streams,[2,25,40,41] fluid shear stress development[10,47] and the respiratory cycle,[48,49] to help identify findings potentially deleterious to favorable long-term clinical outcome.

CFD studies have identified two relevant flow-energy depleting processes within the cavopulmonary pathway of a TCPC:

- collision between the SVC and IVC streams[2,4] and
- viscous dissipation arising from shear stress (friction) acting along the wall of the IVC to RPA conduit.[47]

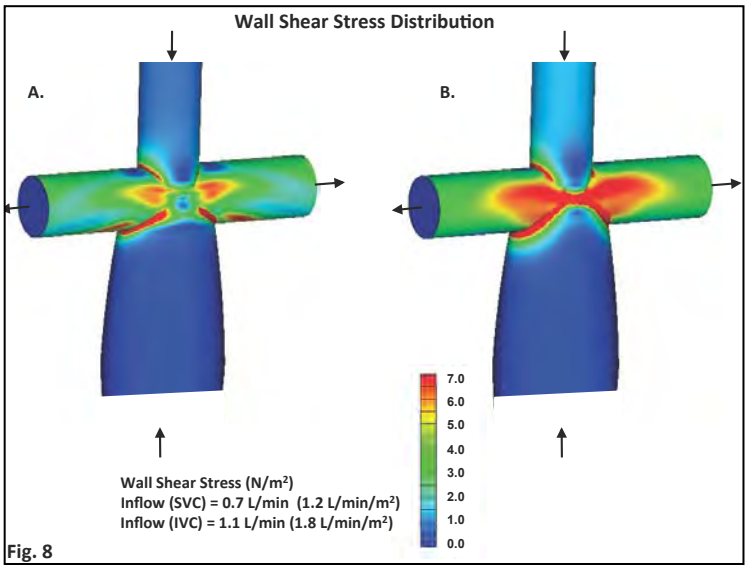

Figure 8. Contour plots of wall shear stress, in N/m², for a completed modified Fontan procedure or TCPC. Incoming (SVC) flow rate is 0.7 L/min (or 1.2 L/min/m²) and incoming (IVC) flow rate is 1.1 L/min (or 1.8 L/min/m²). Representative relative viscosity (η) values are: A. η = 5 and B. η = 8. Incoming (SVC) = outgoing (R-branch) = outgoing (L-branch) = 0.009 m in diameter. Incoming (IVC) = 0.012 m in diameter. The IVC to RPA mid-conduit diameter = .0018 m. The connection of the IVC to the conduit is not shown, to better display the region of mixing between the incoming and outgoing vessels.

To lessen energy loss associated with the former condition, various degrees of caval offsetting and modifications of caval anastomoses have been employed, with some success. However, further reductions in energy loss from the latter process may be more difficult to achieve. Recent studies by Moyle et al.[47] suggest wall shear stress along the extra-cardiac conduit remains the primary determinate of residual cavopulmonary flow-energy wastage.[47] Unfortunately, shear forces are an inevitable byproduct of viscous fluid flowing through confining channels, which may limit surgical options to substantially reduce such energy losses.

Most CFD models of the cavopulmonary pathway assume flow to be steady and continuous, as was done here. However, pulmonary blood flow can contain pulsatile fluctuations and velocity profiles that vary with time, as a consequence of:

- auxillary flow intruding from systemic collateral vessels,[34]
- residual antegrade flow from the main pulmonary artery[2,25] and
- the respiratory cycle.[41,49,50]

Insomuch as the TCPC constitutes an intrathoracic system, incorporating effects from respiration would be expected to have an impact on cavopulmonary blood flow behavior. Hjortal and colleagues[48], for example, measured caval flow rates in TCPC patients using phase-contrast magnetic resonance imaging (MRI). They found SVC flow to remain relatively constant during the respiratory cycle (~1.3L/min/m²); however, IVC flow varied

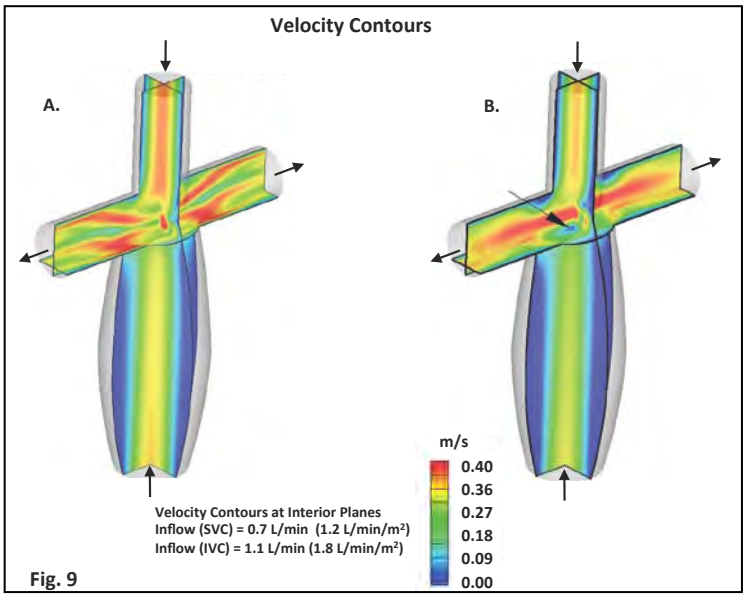

Figure 9. Contour plots of flow velocity magnitudes, in m/s, for the TCPC pathway (Figure 8), as distributed over intersection planes within the vessels. Relative viscosity (η) values are: A. η = 5 and B. η = 8.

substantially (averaging ~1.3L/min/m² with inspiration and ~ 0.8L/min/m² with expiration).

Marsden et al.[49] developed a CFD model of TCPC to accommodate time-dependent cavopulmonary flow. Their studies, although limited to specific Fontan patient anatomy, do demonstrate the potential importance of incorporating simulations of distal pulmonary vessels and affects of respiration on flow, when evaluating flow-energy efficiency. Italani et al.[41] investigated respiratory-driven flow behavior within the extracardiac conduit of TCPCs, using CFD combined with in-vivo caval flow-velocity profiles determined by MRI in modified Fontan patients. During expiration, the model shows SVC flow to penetrate prominently into the conduit, especially with larger-diameter (> 22 mm) conduits. Presumably, the more extensive anastomosis required for the RPA to accommodate a bigger conduit, in conjunction with impaired IVC venous return during expiration, provides SVC flow with an easier passage into the conduit. Alternatively, during inspiration, IVC return tends to dominate flow through the conduit. Larger conduits also permit a greater degree of interplay between caval streams, which can foster energy dissipation and the development of thrombogenic flow patterns. In contrast, smaller-diameter conduits (< 16 mm) tend to lessen SVC-IVC interaction and thus lower the risk of flow stagnation. However, small conduits have been associated with increased dissipative flow-energy loss, likely reflecting wall shear stress' inverse dependence on the cube of the vessel diameter. These types of studies suggest optimal conduit size at the time of completion of the modified Fontan procedure to be 18–22 mm, in patients 3-4 years of age.

Summary

We studied flow energetic - pressure drop (ΔP), energy loss (ΔE) and shear stress development - associated with non-pulsatile (passive)

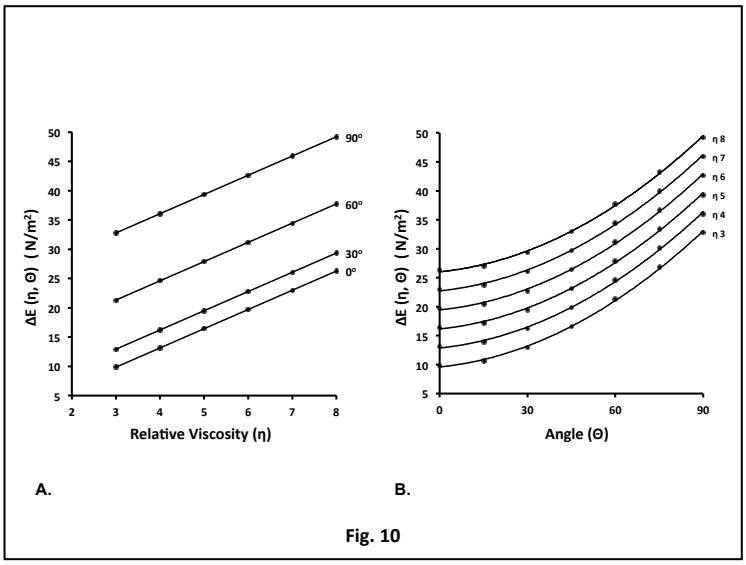

Fig. 10

Figure 10. [A]. Shows flow-energy loss ΔE(η,θ), in N/m², on the y-axis and relative viscosity (η), unitless, on the x-axis, for each angle (θ) of deflection, in degrees. [B]. Shows flow-energy loss ΔE(η,θ), in N/m², on the y-axis and angle (θ) of deflection, in degrees, on the x-axis, for each value of relative viscosity (η). The results for ΔE(η,θ) were determined using the simplified analytical model outlined in Appendix B, eq B.4.

viscous flow undergoing abrupt changes in direction, as encountered in portions of modified Fontan cavopulmonary pathways. Viscosity values reflect clinically-relevant blood hematocrits. The quantities ΔP, ΔE and wall shear stress – determined from numerical solutions to the Navier-Stokes equations – were found to increase significantly with rising fluid viscosity and severity of flow angulation. Fluid pathways were taken to simulate general anatomy associated with operative stages of the modified Fontan procedure. CFD models of flow-energy loss and wall shear stress distribution for Fontan anatomy are reviewed. It is likely that current geometric models may be insufficient to direct Fontan design for more energy-efficient cavopulmonary connections. It is generally believed that maintaining optimal flow-energy utilization in a Fontan circulation will help improve long-term clinical outcome of these challenging patients.

Appendix (A)

Non-pulsatile, incompressible, viscous-fluid flowing in a vessel or conduit was considered to satisfy the overall mechanical energy balance equation:

$$\Delta W_{i,f} = (<P>_i + <K>_i)\, Q_i - (<P>_f + <K>_f)\, Q_f. \qquad (A.1)$$

The quantity $\Delta W_{i,f}$ represents the energy dissipated per time or power loss for the flow transition (i to f). The subscripts (i) and (f) designate the initial (or incoming) and final (or outgoing) portions of the fluid pathway, respectively. Q is the net flow rate. The terms <P> and <K> represents flow-averaged pressure (P) and flow-averaged kinetic energy (K), where:

$$\text{Pressure } <P> = 1/Q \int p\,dq \qquad (A.2a)$$
$$\text{Kinetic Energy } <K> = 1/Q \int \rho/2\, v^2\, dq \qquad (A.2b)$$
$$\text{Flow Rate } Q = \int dq. \qquad (A.2c)$$

Rho (ρ) is the fluid density. Here p and v denote the local pressure (p) and the magnitude of the local velocity (**v**) associated with flow (dq) crossing a differential area (da). The corresponding differential flow satisfies $dq = v_N da$, where v_N is the velocity component normal to da. The symbol (∫) designates summation (weighted by the flow) or integration (with respect to the flow) of p and the elemental kinetic energy $\rho/2\ v^2$, as flow is distributed over the vessel or conduit's cross-sectional area (A). In general, the fluid-pressure distributions and flow-velocity fields will be dissimilar over the entrance and exit areas, A_i and A_f, respectively. Thus, the corresponding bracketed terms $< >_i$ and $< >_f$, in eq. (A.1), which are to be evaluated over A_i and A_f, will take on different values. Equation (A.2a) reflects the rate pressure force performs work on fluid crossing (A); Eq. (A.2b) designates the rate kinetic energy is carried by fluid crossing (A).

The quantity $\Delta W_{i,f}$ may further be written as $\Delta E_{i,f}\, Q_f$, or $\Delta E_{i,f}\, Q_i$ where the flow-energy loss term $\Delta E_{i,f}$ describes the power loss of the fluid system per unit of fluid flow, or the energy loss per unit of fluid volume. Since $Q_i = Q_f$,

$$\Delta E_{i,f} = (<P>_i + <K>_i) - (<P>_f + <K>_f). \qquad (A.3)$$

For the "T" pathway, a bidirectional Glenn shunt, incoming (SVC) flow divides between the two branches (LPA and RPA). Thus,

$$\Delta E_{i,f} = (<P>_i + <K>_i) - \Sigma_{j\,(LPA,RPA)} (<P>_j + <K>_j)\, Q_j / Q_i \qquad (A.4)$$

where (Σ) represents summation, and j enumerates the LPA and RPA for the outgoing mechanical energy.

For the "Cross" pathway, a completed modified Fontan procedure, incoming (SVC) and (IVC) flow distribute between the two branches (LPA and RPA), and

$$\Delta E_{i,f} = \Sigma_{j\,(SVC,\,IVC)} (<P>_j + <K>_j)\, Q_j / Q_i - \Sigma_{j\,(LPA,RPA)} (<P>_j + <K>_j)\, Q_j / Q_i \qquad (A.5)$$

now j enumerates the SVC and IVC for the incoming mechanical energy, and the LPA and RPA for the outgoing mechanical energy.

Appendix (B)

A simplified model can be utilized to help conceptualize the flow-energy loss associated with a fluid of viscosity (η) undergoing an abrupt change in flow angulation (θ). The net energy loss, ΔE(η,θ), is assumed to be composed of a viscous, ΔE(η), and an inertial, ΔE(θ), component. The fluid pathway is considered to consist of three sections, I, II and III, (Figure 1A).

Sections I (incoming) and III (outgoing) are viewed as tubular resistance vessels. The viscous component, ΔE(η), of the energy loss arises as a consequence of shear forces acting within the moving fluid and may be described by a Hagen – Poiseuille type formula, as follows:

$$\Delta E(\eta) = (8\pi\, L/A^2)\eta Q, \qquad (B.1)$$

where L is the net length of sections I and III, A is cross-sectional area, η is fluid viscosity and Q flow rate.

Section II represents the narrow region of the pathway where flow undergoes the abrupt change in direction. The inertial component, ΔE(θ), of the energy loss results from the change in flow velocity (ΔV). Using momentum/energy considerations, and assuming the flow transition to be abrupt, i.e. takes place over an infinitesimal distance, the inertial component of the energy loss can be determined without considering details of the fluid mixing[32], namely:

$$\Delta E(\theta) = \rho/2\, \Delta V^2 = \rho/2\, (V_f^2 + V_i^2 - 2\, V_f\, V_i \cos\theta), \qquad (B.2)$$

where ρ is the fluid density and V_i (V_f) the incoming (outgoing) magnitudes of the flow velocity. The quantity ΔE(θ) represents the kinetic energy of relative motion between the incoming and outgoing fluid streams. Insomuch as there is continuity of flow, $Q = V_i A = V_f A$,

$$\Delta E(\theta) = \rho/A^2\, (1 - \cos\theta) Q^2. \qquad (B.3)$$

Inherent in this approach is that, in the immediate region of flow angulation (Section II), viscosity has insufficient time to significantly influence the flow pattern.*

** Note, the kinetic energy of relative motion ΔE(θ) differs from the overall change in kinetic energy (ΔK) for the fluid transition. For the former, $\Delta E(\theta) = \rho V_i^2 (1-\cos\theta)$ is zero only when θ = 0, i.e. there is no angulation. For the later, $\Delta K = \rho/2\ V_f^2 - \rho/2\ V_i^2$ is zero when the magnitude of $V_f = V_i$.*

Thus, the net flow-energy loss for the overall fluid transition becomes:

$$\Delta E(\eta,\theta) = (8\pi L/A^2)\eta Q + \rho/A^2 (1 - \cos\theta)Q^2. \qquad (B.4)$$

With low viscosity, the inertial term tends to dominate; whereas, for high viscosity the viscous term is most important. Figure 10 shows net flow energy loss ΔE (η,θ) as a function of viscosity η and angle (θ) of deflection, based on equation B.4. Note, the macroscopic energy balance considered here gives the total dissipated energy. However, no information is provided on whether the dissipation is uniform or homogenous within the fluid. CFD provides this missing information.

References

1. Kao JM, Alejos JC, Grant PW, Williams RG, Shannon KM, Laks H (1994) Conversion of atriopulmonary to cavopulmonary anastomosis in management of late arrhythmias and atrial thrombosis. Ann Thorac Surg 58:1510-1514.
2. de Leval MR, Dubini G, Migliavacca F, Jalali H, Camporini G, Redington A, Pietrabissa R (1996) Use of computational fluid dynamics in the design of surgical procedures: Application to the study of competitive flows in cavopulmonary connections. J Thorac Cardiovasc Surg 111:502-513.
3. Stein DG, Laks H, Drinkwater DC, Permut LC, Louie HW, Pearl JM, George BL, Williams RG (1991) Results of total cavopulmonary connection in the treatment of patients with a functional single ventricle. J Thorac Cardiovasc Surg Aug; 102(2): 280-6.
4. de Leval MR, Kilner P, Gewillig M, Bull C (1988) Total cavopulmonary connection: A logical alternative to atriopulmonary connection for complex Fontan operations: Experimental studies and early clinical experience. J Thorac Cardiovasc Surg 96:682-695.
5. Kim Yh, Walker PG, Fontaine AA, Panchal S, Ensley AE, Oshinski J, Sharma S, Ha B, Lucas CL, Yoganathan AP (1995) Hemodynamics of the Fontan connection: An invitro study. J Biomech Eng 117:423-428.
6. Sharma S, Goudy S, Walker P, Panchal S, Ensley A, Kanter K, Tam V, Fyfe D, Yoganathan A (1996) *In vitro* flow experiments for determination of optimal geometry of total cavopulmonary connection for surgical repair of children with functional single ventricle. J Am Coll Cardiol 27:1264-1269.
7. Fogel MA, Weinberg PM, Hoydu A, Hubbard A, Rychik J, Jacobs M, Fellows KE, Haselgrove J (1997) The nature of flow in the systemic venous pathway measured by magnetic resonance blood tagging in patients having the Fontan operation. J Thorac Cardiovasc Surg 114:1032-1041.
8. Kim SH, Park YH, Cho BK (1997) Hemodynamics of the total cavopulmonary connection: An *in vitro* study. Yonsei Med J 38:33-39.
9. Be'eri E, Maier SE, Landzberg MJ, Chung T, Geva T (1998) In vivo evaluation of Fontan pathway flow dynamics by multidimensional phase-velocity magnetic resonance imaging. Circulation 98:2873-2882.
10. Ensley AE, Lynch P, Chatzimavroudis GP, Lucas C, Sharma S, Yoganathan AP (1999) Toward designing the optimal total cavopulmonary connection: An *in vitro* study. Ann Thorac Surg 68:1384-1390.
11. Ensley AE, Ramuzat A, Healy TM, Chatzimavroudis GP, Lucas C, Sharma S, Pettigrew R, Yoganathan AP (2000) Fluid mechanic assessment of the total cavopulmonary connection using magnetic resonance phase velocity mapping and digital particle image velocimetry. Ann Biomed Eng 28:1172-1183.
12. Ryu K, Healy TM, Ensley AE, Sharma S, Lucas C, Yoganathan AP (2001) Importance of accurate geometry in the study of the total cavopulmonary connection: Computational simulations and *in vitro* experiments. Ann Biomed Eng 29:844-853.
13. Sharma S, Ensley AE, Hopkins K, Chatzimavroudis GP, Healy TM, Tam VKH, Kanter KR Yoganathan AP (2001) *In vivo* flow dynamics of the total cavopulmonary connection from three-dimensional multislice magnetic resonance imaging. Ann Thorac Surg 71:889-898.
14. Healy TM, Lucas C, Yoganathan AP (2001) Noninvasive fluid dynamic power loss assessments for total cavopulmonary connections using the viscous dissipation function: A feasibility study. J Biomech Eng 123:317-324.
15. DeGroff CG, Carlton JD, Weinberg CE, Ellison MC, Shandas R, Valdes-Cruz L (2002) Effect of vessel size on the flow efficiency of the total cavopulmonary connection: *In vitro* studies. Pediatr Cardiol 23:171-177.
16. DeGroff CG, Shandas R (2002) Designing the optimal total cavopulmonary connection: Pulsatile versus steady flow experiments. Med Sci Monitor 8:MT41-MT45.
17. Van Haesdonck J-M, Mertens L, Sizaire R, Montas G, Purnode B, Daenen W, Crochet M, Gewillig M (1995) Comparison by computerized numeric modeling of energy losses in different Fontan connections. Circulation 92:322-326.
18. Migliavacca F, de Leval MR, Dubini G, Pietrabissa R, Fumero R (1999) Computational fluid dynamic simulations of cavopulmonary connections with an extracardiac lateral conduit. Med Eng Phys 21:187-193.
19. Bove EL, de Leval MR, Migliavacca F, Guadagni G, Dubini G (2003) Computational fluid dynamics in the evaluation of hemodynamic performance of cavopulmonary connections after the Norwood procedure for hypoplastic left heart syndrome. J Thorac Cardiovasc Surg 126:1040-1047.
20. Migliavacca F, Dubini G, Bove EL, de Leval MR (2003) Computational fluid dynamics simulations in realistic 3-D geometries of the total cavopulmonary anastomossis: The influence of the inferior caval anastomosis. J Biomech Eng 125:805-813.
21. Amodeo A, Grigioni M, D'Avenio G, Daniele C, Di Donato RM (2004) The patterns of flow in the total extracardiac cavopulmonary connection. Cardiol Young 14(Suppl 3):53-56.
22. Dubini G, Migliavacca F, Pennati G, de Leval MR, Bove EL (2004) Ten years of modeling to achieve haemodynamic optimization of the total cavopulmonary connection. Cardiol Young 14(Suppl 3): 48-52.
23. Hsia T-Y, Migliavacca F, Pittaccio S, Radaelli A, Dubini G, Pennati G, de Leval M (2004) Computational fluid dynamic study of flow optimization in realistic models of the total cavopulmonary connections. J Surg Res 116:305-313.
24. Liu Y, Pekkan K, Jones SC, Yoganathan AP (2004) The effects of different mesh generation methods on computational fluid

dynamic analysis and power loss assessment in total cavopulmonary connection. J Biomech Eng 126:594-603.
25. Migliavacca F, Pennati G, Dubini G, de Leval MR (2004) A study of mathematical modeling of the competitions of flow in the cavopulmonary anastomosis with persistent forward flow. Cardiol Young 14(Suppl 3):32-37.
26. DeGroff C, Birnbaum B, Shandas R, Orlando W, Hertzberg J (2005) Computational simulations of the total cavopulmonary connection: Insights in optimizing numerical solutions. Med Eng Phys 27:135-146.
27. Pekkan K, de Zelicourt D, Ge L, Sotiropoulos F, Frakes D, Fogel MA, Yoganathan AP (2005) Physics-driven CFD modeling of complex anatomical cardiovascular flows-a TCPC case study. Ann Biomed Eng 33:284-300.
28. Socci L, Gervaso F, Migliavacca F, Pennati G, Dubini G, Ait-Ali L, Festa P, Amoretti F, Scebba L, Luisi VS (2005) Computational fluid dynamics in a model of the total cavopulmonary connection reconstructed using magnetic resonance images. Cardiol Young 15(Suppl 3):61-67.
29. Wiesman JP, Ross-Ascuitto NT, Gaver DP, Ascuitto RJ (2005) A computational investigation of flow-mechanical energy loss: Relevance to the total cavopulmonary connection. Comsol Multiphysics 411-416.
30. Orlando W, Shandas R, DeGroff C (2006) Efficiency differences in computational simulations of the total cavopulmonary circulation with and without compliant vessel walls. Comput Meth Prog Biomed 81:220-227.
31. DeGroff (2008) Modeling the Fontan Circulation: Where We Are amd Where We Need to Go. Pediatr Cardiol 29:3-12.
32. Ascuitto RJ, Kydon DW, Ross-Ascuitto NT (2001) Pressure loss from flow energy dissipation: Relevance to Fontan-type modifications. Pediatr Cardiol 22:110-115.
33. Ascuitto RJ, Kydon DW, Ross-Ascuitto NT (2003) Streamlining fluid pathways lessens flow energy dissipation: Relevance to atriocavopulmonary connections. Pediatr Cardiol 24:249-258.
34. Ascuitto RJ, Ross-Ascuitto NT (2004) Systematic-to-pulmonary collaterals: A source of flow energy loss in Fontan physiology. Pediatr Cardiol 25:472-481.
35. Wiesman JP, Gaver DP, Ross-Ascuitto NT, Ascuitto RJ (2006) Energy-depleting fluid-flow disturbances associated with small pressure change: Relevance to obstructed total cavopulmonary connections. Congenital Cardiology Today (International Edition) 4, 7:1-11.
36. Ascuitto R, Ross-Ascuitto N, Guillot M (2010) Fluid Viscosity Increases Pressure Drop and Exacerbates Flow-Energy Loss (Relevance to Modified-Fontan Patients with Elevated Hematocrit). Congenital Cardiology Today Vol 8, Issue 12.
37. Nygard KK, Wilder M, Berkson J (1935) The relation between viscosity of the blood and the relative volume of erythrocytes (hematocrit value). Amer J Physiol 114:128-131.
38. Wells RE Jr, Merrill EW (1962) Influence of flow properties of blood upon viscosity-hematocrit relationships. J Clin Invest 41:1591-1598.
39. Alexi-Meskishvili V, Ovroutski S, Ewert P, Dahnert I, Berger F, Lange PE, Hetzer R (2000) Optimal conduit size for extracardiac Fontan operation. European J of Cardio-Thorac Surg 18:690-695.
40. Lardo AC, Webber SA, Friehs I, Del Nido PJ, Cape EG (1999) Fluid dynamic comparison of intra-atrial and extracardiac total cvopulmonary connections. J Thorac Cardiovasc Surg 117:697-704.
41. Itatani K, Miyaji K, Tomoyasu T, Nakahata Y, Ohara K, Takamoto S, Ishii M (2009) Optimal Conduit Size of the Extracardiac Fontan Operation Based on Energy Loss and Flow Stagnation. Ann Thorac Surg 888:565-73.
42. Fontan F, Baudet E. Surgical repair of tricuspid atersia. Thorax 1971; 26:240-248.
43. Puga FG, Chiavarelli M, Hagler DJ (1987) Modifications of the Fontan operation applicable to patients with left atrioventricular valve atresia or single atrioventricular valve. Circulation 76:III53-III60.
44. Pearl JM, Laks H, Stein DG, Drinkwater DW, George BL, Williams RG (1991) Total cavopulmonary anastomosis vs. conventional modified Fontan procedur. Ann Thorac Surg 52:180-196.
45. Waniewski J, Kurowska W, Mizerski J, Trykozko A, Nowinski K, Brzezinska-Rajszys G, Kosciesza A (2005) The Effects of Graft Geometry on the Patency of a Systemic-to-Pulmonary Shunt: A computational Fluid Dynamics Study. Artif Organs 29(8):642-650.
46. Pennati G, Fiore GB, Migliavacca F, Lagana K, Fumero R, Dubini G. In vitro steady-flow analysis of systemic-to-pulmonary shunt haemodynamics. J Biomech 2001;34:23-30.
47. Moyle KR, Mallinson GD, Occleshaw CJ, Cowan BR, Gentles TL (2006) Wall Shear Stress is the Primary Mechanism of Energy Loss in the Fontan Connection. Pediatr Cardiol 27:309-315.
48. Hjortdal VE, Emmertsen K, Stenberg E, etal (2003) Effects of exercise and respiration on blood flow in total cavopulmonary connection: a real-time magnetic resonance flow study. Circulation 108:1227-1231.
49. Marsden AL, Vignon-Clementel IE, Chan FP, Feinstein JA, Taylor CA (2007) Effects of exercise and respiration on hemodynamic efficiency in CFD simulations of the total cavopulmonary connection. Ann Biomed Eng 35:250-263.
50. Pedersen EM, Stenbog EV, Frund T, etal (2002) Flow during exercise in the total cavopulmonary connection measured by magnetic resonance velocity mapping. Heart 87:554-558.

CCT

51

Corresponding Author:

Robert Ascuitto, PhD, MD
Department of Pediatrics
Division of Cardiology
Louisiana State University Health Sciences Center
New Orleans, LA, 70112 USA
and
Children's Hospital of New Orleans
Division of Cardiology
New Orleans, LA 70118 USA
nrossascuitto@yahoo.com

Martin Guillot, PhD
Department of Mechanical Engineering
University of New Orleans
New Orleans, LA 70148

Nancy Ross-Ascuitto MD
Department of Pediatrics
Division of Cardiology
Louisiana State University Health Sciences Center
New Orleans, LA, 70112 USA
and
Children's Hospital of New Orleans,
Division of Cardiology
New Orleans, LA 70118 USA

Hope for Hearts Everywhere: An Introduction to Harboring Hearts

By Michelle Javian, Co-Founder & Executive Director, Harboring Hearts

It is a well-known fact that heart disease is the leading cause of death in America for both men and women, claiming the lives of more than one in four people every year. Less well known, but just as important, are the individual stories of the multitudes of families and friends of each and every heart disease victim. These victims and their families often bear immense emotional and financial burdens, and many of them find themselves with nowhere to turn for help. Michelle Javian and Yuki Kotani, both of whom have their own personal experiences with loved ones and heart disease, have made it their personal mission to help these sometimes overlooked families in whatever way they can. As a result, they founded Harboring Hearts as a non-profit organization in 2009 and have been making a difference in the cardiac disease community ever since.

Harboring Hearts is a 501(c)3 non-profit organization dedicated to helping meet the needs of the families of cardiac patients. Our mission is to provide heart patients and their families the support of a home-like haven and a nurturing community of resources, a community comprised of heart patients, their families, and others impacted by heart disease. Specifically, our vision is to expand upon the housing concept by providing not only assistance with the immediate needs of accommodation, but also emotional support to help people understand that they can continue to lead rewarding lives during and after heart disease. In these ways, Harboring Hearts is revolutionalizing the heart community, one family at a time.

What sets Harboring Hearts apart is the personal dedication of its founders. Co-founder Michelle's father passed away after complications arose from a heart transplant. Yuki Kotani's father was also affected by heart disease, although fortunately survived, while Yuki herself is a congenital heart defect survivor. It was during their respective trials with heart disease that they both recognized the great need for a vibrant community of support for the families of patients, who are often seeking treatment far from home. It did not take long after Michelle and Yuki met for them to recognize their shared experiences and decide to combine their efforts toward creating a solution. The result of their friendship became Harboring Hearts, which, coincidentally—or not so coincidentally—officially received its 501(c)3 status on the anniversary of the passing of Michelle's father.

> ***"The goal of Harboring Hearts has been to provide emotional and financial support to as many families as possible."***

In light of the realities of cardiologic treatment, the need for an organization such as Harboring Hearts is clear. Expenses vary among medical procedures—anywhere from $30,000 to over $450,000 for a single treatment—but in virtually all instances constitute a tremendous financial burden to patients and their families. By the time they are in need of a life-saving procedure, many have already experienced astronomical medical bills. On average, 50% of the families of those afflicted with heart disease make less than $50,000 a year. From these statistics, it goes without saying that the majority of heart patients and their families will need crucial financial and emotional support. This is where Harboring Hearts steps in. "Harboring Hearts Housing is a necessary organization because the costs of staying at the hospital in New York City is anywhere from $700 – $900 per night for a patient," William Sullivan, CEO and President of the Ronald McDonald House of New York City says. "In addition, many cardiac patients that live outside of New York City will have to spend a substantial amount of time and money traveling to and from the hospital. Having a temporary home close to the hospital during the patient's treatment will substantially help families during these trying times."

Photo Credit: Suzanne DeChillo/The New York Times.

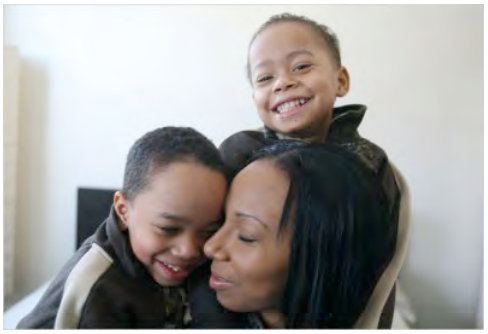

Photo Credit: Emily Anne Epstein/Metro.

Left: Yuki Kotani; right: Michelle Javian

The goal of Harboring Hearts has been to provide emotional and financial support to as many families as possible. Megan Sterrett, Principal of Doshi Capital Partners and Heritage Capital India, echoes this sentiment, saying, "My first-hand experience watching my grandfather undergo cardiac

"We frequently invite doctors as keynote speakers at many of our events...."

treatments made me realize how important Harboring Hearts' mission is to others. Harboring Hearts provides an essential component to the well being of both the heart patients and their families – support." Since its founding, this charity has donated thousands of dollars, money raised mostly through various fundraising events such as golf tournaments, Hamptoms benefits, and masquerade balls. Backed by enthusiastic and growing support, Harboring Hearts has been able to help more than 200 people needing the same support Michelle, Yuki, and their families once did. Leslie, Johan, and Tariq Lopez are one such family.

Leslie Lopez had already seen one daughter's life taken by cardiomyopathy in 2002. When her sons, four year-old twins Johan and Tariq, were diagnosed with the same disease in 2007, they joined the daunting list of over 100,000 people in the United States waiting for a heart transplant. Leslie, who lived with her children in Trinidad at the time, was advised by doctors to visit New York to consult with specialists. After a lengthy ordeal of traveling and tests, the boys received much-needed heart transplants at the Morgan-Stanley Children's Hospital of New York-Presbyterian in 2008. The transplants gave them a miraculous second chance to live, but their struggle was far from over: the little family found themselves with hardly any money left to afford a place to live while the boys completed follow-up tests. After months of living in the New York City shelter system—which posed a significant risk to the twins' vulnerable immune systems—they connected with Harboring Hearts to receive help. Leslie, Tariq, and Johan were not only provided with a safe, clean place to live while treatments continued, but also enjoyed routine contact with the Harboring Hearts team. Leslie and her children are just one of many who have found a literal safe haven in Harboring Hearts.

Once a patient is admitted into a hospital, they and their family are paired with a social worker, who collaborates efficiently with Harboring Hearts to provide assistance tailored to the circumstances of individual families. Medical professionals can also play a very important role our cause. Harboring Hearts works closely with several hospitals in the New York City area—such as New York Presbyterian Hospital—and are always looking to create closer ties with other facilities to provide social workers with strong referrals for their clients. Details about the many events we host throughout the year can be found on our website, and our doors are always open for interested medical professionals.

We frequently invite doctors as keynote speakers at many of our events, lending professional experience to the Harboring Hearts community while also providing the featured speaker a unique honor and opportunity. We are finding ways to increase our influence through social media outlets and encourage the participation of healthcare employees and patients in this effort.

There is additional potential for leadership opportunities on our steadily growing Board of Directors. The support that the medical community provides to Harboring Hearts has become an essential ingredient in the success of our endeavors. Above all, increased awareness of the Harboring Hearts cause will provide a positive impact on the cardiac community. For more information on how to join us in our mission of providing support to heart patients and their families, please visit our website at www.harboringhearts.org. Together we can continue to give hope to hearts everywhere.

CCT

Watch Video about Harboring Hearts
www.youtube.com/watch?v=NLs4-YvRH_k

Michelle Javian, Co-Founder & Executive Director
Harboring Hearts
333 West 52nd St, Fl. 7
New York, NY 10019 USA
Phone: 516.816.3893
Fax: 212.255.8371

michelle.javian@harboringhearts.org
www.HarboringHearts.org
On Twitter: @HarboringHearts
On Facebook: www.facebook.com/harboringhearts

CONGENITAL CARDIOLOGY TODAY

CALL FOR CASES AND OTHER ORIGINAL ARTICLES

Do you have interesting research results, observations, human interest stories, reports of meetings, etc. to share?

Submit your manuscript to:
RichardK@CCT.bz

- Title page should contain a brief title and full names of all authors, their professional degrees, and their institutional affiliations. The principal author should be identified as the first author. Contact information for the principal author including phone number, fax number, email address, and mailing address should be included.
- Optionally, a picture of the author(s) may be submitted.
- No abstract should be submitted.
- The main text of the article should be written in informal style using correct English. The final manuscript may be between 400-4,000 words, and contain pictures, graphs, charts and tables. Accepted manuscripts will be published within 1-3 months of receipt. Abbreviations which are commonplace in pediatric cardiology or in the lay literature may be used.
- Comprehensive references are not required. We recommend that you provide only the most important and relevant references using the standard format.
- Figures should be submitted separately as individual separate electronic files. Numbered figure captions should be included in the main Word file after the references. Captions should be brief.
- Only articles that have not been published previously will be considered for publication.
- Published articles become the property of the Congenital Cardiology Today and may not be published, copied or reproduced elsewhere without permission from Congenital Cardiology Today.

New Heart Cells Increase by 30% After Stem Cell Infusion, UB Research Shows

Healthy, new heart cells have been generated by animals with chronic Ischemic Heart Disease after receiving stem cells derived from cardiac biopsies or "cardiospheres," according to research conducted at the University at Buffalo School of Medicine and Biomedical Sciences.

The research was presented on November 15th at the Scientific Sessions of the American Heart Association in Orlando.

The UB research demonstrated a 30% increase in healthy heart muscle cells within a month after receiving cardiosphere-derived cells (or CDCs). This finding is contrary to conventional wisdom which has held that heart cells are terminally differentiated and thus, are unable to divide.

Ischemic heart disease from coronary artery narrowing and prior heart attacks is the most common cause of heart failure, the UB researchers explain. While other investigators have largely focused on regenerating muscle in scarred tissue, the UB group has shown that cardiac repair could be brought about by infusing the CDCs slowly into coronary arteries of the diseased as well as normal areas of the heart.

"Whereas most research has focused upon irreversible damage and scarring following a heart attack, we have shown that a single CDC infusion is capable of improving heart function in areas of the heart that are viable but not functioning normally," explains study co-author John M. Canty Jr., MD, the Albert and Elizabeth Rekate Professor of Medicine in the UB medical school and UB's chief of cardiovascular medicine. He explains that areas of myocardial dysfunction without fibrotic scarring are common in patients with heart failure from coronary artery disease and that they arise from remodeling in response to a heart attack, as well as adaptations that develop from periods of inadequate blood flow, sometimes called hibernating myocardium.

"The rationale for our approach is somewhat analogous to planting seeds in fertile soil versus trying to grow plants in sand," Canty comments.

"We have shown that cells derived from heart biopsies can be expanded outside of the body and slowly infused back into the coronary arteries of animals with chronic dysfunction from restricted blood flow or hibernating myocardium," says Gen Suzuki, MD, Research Assistant, Professor of Medicine in the UB Medical School, and lead author on the research. "The new cardiac muscle cells are small and function more normally than diseased large, hypertrophied myocytes."

Canty adds that infusing stem cell formulations directly into coronary arteries also delivers the cells throughout the heart and is much simpler than injecting cells directly into heart muscle which requires equipment that is not widely available.

The research currently is in a preclinical phase but the UB researchers expect that translation to determine effectiveness in patients could take place within two to three years or possibly even sooner.

Co-authors on the paper are Thomas Cimato, MD, PhD, Assistant Professor of Medicine and Merced Leiker, Research Associate in the UB Division of Cardiovascular Medicine.

The research was funded by the Department of Veterans Affairs; the Empire State Stem Cell Board; the National Heart, Lung and Blood Institute of the National Institutes of Health; and the Albert and Elizabeth Rekate Fund.

Patients with Hypertrophic Cardiomyopathy Live into Their 90's

Hypertrophic cardiomyopathy (HCM) is consistent with survival to normal life expectancy, including particularly advanced age into the tenth decade of life, with demise ultimately largely unrelated to this disease, according to a study presented November 13th at the American Heart Association (AHA) scientific sessions in Orlando, Fla.

HCM is the most common cause of sudden death in the young, but survival to a particularly advanced age is less well understood.

"In the past, this disease has been associated with a grim prognosis, due to the deadly nature in young people, but we have learned through this analysis that those assumptions were inaccurate," said the study's lead author Barry J. Maron, MD, Director of the Hypertrophic Cardiomyopathy Center at the Minneapolis Heart Institute Foundation. "We are continuing to learn about this unique disease state."

In the study, Maron and colleagues assessed the prevalence, clinical features and demographics of HCM patients surviving to the age of 90 years or older through an interrogation of the Minneapolis Heart Institute Foundation's HCM Center database.

Of the 1,297 HCM patients, 26 had achieved the age of at least 90 years; 69% were women. The age at which HCM was diagnosed ranged from 61 to 92 years, with disease recognition under fortuitous circumstances by detection of a heart murmur or during family screening (six patients), or after onset of new symptoms (20 patients).

At the most recent evaluation (or death) patients were 90.0 to 96.7 years of age, with six presently alive at 90 to 96 years of age. Maron noted that HCM did not appear to be the primary cause of demise in any patient.

HCM-related complications occurred in 18 patients, including heart failure symptoms, atrial fibrillation and non-fatal embolic stroke. Although no patient died suddenly, 13 still carried conventional HCM markers of risk.

Interestingly, a greater proportion of these HCM patients reached the age 90 years of older (2%) than expected in the general population (0.8%).

"We showed that hypertrophic cardiomyopathy—the most common cause of death among young people—is associated not only with normal life, but also extended longevity," Maron said. "These findings underscore a principle of the disease that has been falsely assumed;

namely, that this disease will lead to an early demise in all patients."

Finally, these data can reassure mainly patients who are diagnosed with HCM that their lives will not necessarily be cut short, Maron concluded.

Families Report Adverse Events in Hospitalized Children not Tracked by Healthcare Providers

Families of hospitalized children can provide valuable information about adverse events relating to their children's care that complements information documented by healthcare professionals, states a study published in *CMAJ* (*Canadian Medical Association Journal*)

Hospitals in Canada have instituted systems to encourage reporting of adverse events — things that may negatively affect the recovery or health of a patient — in patient care. In pediatrics, it is estimated that 1% of children in hospital experience an adverse event and 60% of these are preventable. However, there is lower reporting of these events by health care professionals compared with those documented on charts.

Researchers from British Columbia conducted a study to determine whether an adverse event system involving families would result in a change in events reporting by health care providers. The researchers expected that reporting rates would increase and that families would provide useful information on patient safety.

The study included 544 families whose children were on an inpatient ward that provided general medical, general surgical, neurologic or neurosurgical care in British Columbia's Children's Hospital to babies, children and adolescents. Each family submitted a report and of these 544 participants, 201 (37%) noted at least one adverse event or near miss during hospitalization, for a total of 321 adverse events. Adverse events included medication problems such as a reaction or incorrect dosage, treatment complications, equipment problems and miscommunication. Most of these events — 313 out of 321 — were not reported by the hospital.

However, "the results of this study showed that the introduction of a family-initiated adverse event reporting system administered at the time of discharge from a pediatric inpatient surgical ward was not associated with a change in the rate of reporting of adverse events by health care providers," writes Dr. Jeremy Daniels, University of British Columbia, with coauthors.

Only 2.5% of the events noted by families were documented by health care providers, although "almost half of the adverse events reported by families represented valid safety concerns, not merely reports of dissatisfaction," states the authors. In 139 cases, families received apologies for these incidents.

"The initiation of [the] family-based patient safety reporting system provided new opportunities to learn and improve the safety of health care provision without an additional reporting burden for health care providers," write the authors. "Giving families the opportunity to report patient safety events did not remove the barriers to reporting by providers (time pressure, culture of blame, fear of reprisal and lack of belief in the value of reporting) but served to complement such reporting."
The authors conclude that "further research is needed to delineate how best to harness the potential of families to improve the safety of the health care system."

In a related commentary www.cmaj.ca/site/embargo/cmaj111311.pdf, Drs. Charles Vincent and Rachel Davis, Imperial Centre for Patient Safety & Service Quality, Imperial College, London, UK, state that "paying close attention to patients' and families' experience of care and their reports of safety issues may be the best early warning system we have for detecting the point at which poor care deteriorates into care that is clearly dangerous."

White Pediatric Heart Transplant Patients More Likely Than Non-whites to Survive Long-term

Johns Hopkins research finds racial, gender disparities among those living 10 years after surgery.

White heart transplant patients under the age of 18 are more than twice as likely to be alive a decade after surgery as their African-American counterparts, new Johns Hopkins research suggests.

The findings, part of a large-scale review of factors that appear to significantly influence long-term survival among pediatric heart transplant patients, was presented at the American Heart Association's annual Scientific Sessions in Orlando.

"It's unclear whether these racial disparities are due to biological differences or socio-economic differences that have an impact on access to care, or some combination of the two," says Arman Kilic, MD, a surgical resident at The Johns Hopkins Hospital in Baltimore who is scheduled to make the AHA presentation. "That's been hotly debated, but these data tell us we need to do a lot more research to figure out why those disparities exist and how we can narrow the gap."

Kilic analyzed United Network of Organ Sharing (UNOS) data from the 2,721 pediatric heart transplants performed in the United States between 1987 and 1999. Forty-two percent of patients (1,143) were alive 10 years or more after transplant. The average age of the recipients at the time of transplant was less than six years.

In addition to racial disparities in longterm survival, the analysis also showed that boys are 26% more likely than girls to survive a decade after their transplants; and children who had their surgeries at hospitals where large numbers of transplants are done annually were more likely to be alive 10 years later. For every 10 additional pediatric heart transplants conducted at a hospital each year, the chance of 10-year survival for patients transplanted there increased 36 percent. Patients at high-volume centers do better not only because their surgeons likely have more experience with heart transplants, Kilic says, but also because the staff and facilities are likely better equipped to manage the complex post-operative care of these patients.

The findings also show that patients transplanted later in the study period and those who got their hearts from younger donors were also significantly more likely to survive long term. Those who were on mechanical ventilation prior to their transplant were less likely to live a decade than those who were breathing on their own before surgery.

"Children are potentially a group of patients whose survival after transplantation could

be several decades, so it's especially important to better understand why some do well and others do not," Kilic says.

Diseased Hearts to Heal Themselves in Future

Oncostatin M regulates the reversion of heart muscle cells into precursor cells and is vitally important for the self-healing powers of the heart.

Cellular reversion processes arise in diseases of the heart muscle, for example myocardial infarction and cardiomyopathy, which limit the fatal consequences for the organ. Scientists from the Max Planck Institute for Heart and Lung Research in Bad Nauheim and the Schüchtermann Klinik in Bad Rothenfelde have identified a protein which fulfills a central task in this reversion process by stimulating the regression of individual heart muscle cells into their precursor cells. It is now planned to improve the self-healing powers of the heart with the help of this protein.

In order to regenerate damaged heart muscle as caused by a heart attack, for example, the damaged muscle cells must be replaced by new ones. The number of cells to be replaced may be considerable, depending on the extent of the damage caused. Simpler vertebrates like the salamander adopt a strategy whereby surviving healthy heart muscle cells regress into an embryonic state. This process, which is known as dedifferentiation, produces cells which contain a series of stem cell markers and re-attain their cell division activity. Thus, new cells are produced which convert, in turn, into heart muscle cells. The cardiac function is then restored through the remodelling of the muscle tissue.

An optimised repair mechanism of this kind does not exist in humans. Although heart stem cells were discovered some time ago, exactly how and to what extent they play a role in cardiac repair is a matter of dispute. It has only been known for a few years that processes comparable to those found in the salamander even exist in mammals.

Thomas Braun's research group at the Max Planck Institute for Heart and Lung Research in Bad Nauheim has now discovered the molecule responsible for controlling this dedifferentiation of heart muscle cells in mammals. The scientists initially noticed the high concentration of oncostatin M in tissue

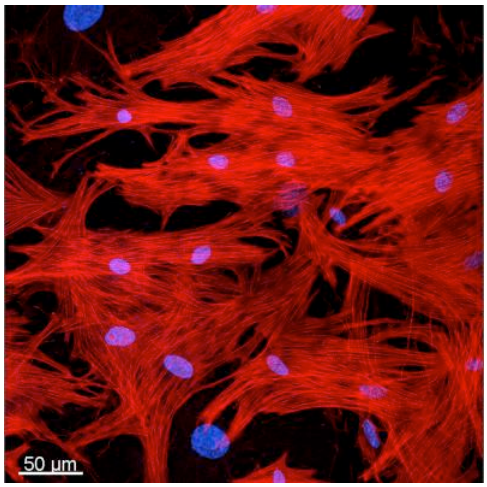

Cellular regression in diseased heart tissue with the help of oncostatin M: The image shows heart muscles under the fluorescence microscope. The myofibrils are stained red, the cell nuclei blue. Credit: MPI for Heart and Lung Research.

samples from the hearts of patients suffering from myocardial infarction. It was already known that this protein is responsible for the dedifferentiation of different cell types, among other things. The researchers therefore treated cultivated heart muscle cells with oncostatin M in the laboratory and were then able to trace the regression of the cells live under the microscope: "Based on certain changes in the cells, we were able to see that almost all heart muscle cells had been dedifferentiated within six days of treatment with oncostatin M," explains Braun. "We were also able to demonstrate the presence of various stem cell markers in the cells. This should be understood as an indicator that these cells had been switched to a repair mode."

Using a mouse infarct model, the Max Planck researchers succeeded in demonstrating that oncostatin M actually does stimulate the repair of damaged heart muscle tissue as presumed. One of the two test groups had been modified genetically in advance to ensure that the oncostatin M could not have any effect in these animals. "The difference between the two groups was astonishing. Whereas in the group in which oncostatin M could take effect almost all animals were still alive after four weeks, 40% of the genetically modified mice had died from the effects of the infarction," says Braun. The reason for this was that oncostatin M ensured clearly quantifiable better cardiac function in the unmodified animals.

The scientists in Bad Nauheim would now like to find a way of using oncostatin M in treatment. The aim is to strengthen the self-healing powers of the damaged heart muscle and to enable the restoration of cardiac function for the first time. The downside, however, is that oncostatin M was also observed to be counterproductive and exacerbated the damage in an experiment on a chronically diseased heart. "We believe that oncostatin M has considerable potential for efficiently healing damaged heart muscle tissue. What we now need is to be able to pinpoint the precise window of application to prevent any possible negative effects," says Braun.

Original publication: Thomas Kubin, Jochen Pöling, Sawa Kostin, Praveen Gajawada, Stefan Hein, Wolfgang Rees, Astrid Wietelmann, Minoru Tanaka, Holger Lörchner, Silvia Schimanski, Marten Szibor, Henning Warnecke, Thomas Braun: Oncostatin M Is a Major Mediator of Cardiomyocyte Dedifferentiation and Remodeling. Cell Stem Cell 9, 420, 201.

Adult Congenital Patients Are Increasingly Being Treated in Pediatrics Hospitals

Higher surgical costs for adult congenital heart patients is associated with higher rates of inpatient death compared to surgical admissions that incur lower costs, according to a study in *Circulation: Quality and Outcomes*, a journal of the American Heart Association.

In the study, researchers sought to understand resource use by adults undergoing congenital heart surgery in pediatric hospitals, analyze the association between high resource use and inpatient death, and identify risk factors for high resource use.

They found that although the number of adults undergoing congenital heart surgery in pediatric hospitals is increasing, adult congenital heart patients are not using a disproportionate amount of the hospitals' resources.

The researchers identified five factors that are associated with higher inpatient charges: greater surgical complexity, government insurance, DiGeorge Syndrome, weekend admission and depression. DiGeorge Syndrome is a genetic disorder affecting the thymus and thyroid that also causes heart defects.

With the vast majority of congenital heart patients surviving to adulthood, adults now outnumber pediatric congenital heart patients. Many adult patients with congenital heart disease continue to receive their medical, interventional and surgical care at pediatric hospitals.

"The most interesting and actionable of our findings was that depression is a risk factor for high resource use among this surgical population. While we cannot change a patient's surgery complexity or presence of DiGeorge Syndrome, we might be able to implement a treatment strategy for a potentially modifiable risk factor such as depression. One could imagine implementing a screening and treatment program for depression and assessing its impact in inpatient resource use," said Oscar J. Benavidez, MD, lead author of the study and now chief of the Division of Pediatric-Congenital Cardiology at Massachusetts General Hospital in Boston. The study was done when he was at Children's Hospital Boston. "We might not only lower resource use but also save lives."

Benavidez and colleagues analyzed patient information at 42 pediatric hospitals in the United States from 2000 to 2008. Findings from the study include:

- Adults make up 3.1% of congenital heart surgery admissions to pediatric hospitals, but account for only 2.2% of total hospital charges.
- Although high resource use admissions made up 10% of adult admissions, they accounted for 34% of charges for all adult congenital heart surgery admissions.
- The rate of death is 16% for the most costly patients, but only 0.7 % for other adult congenital heart patients.
- Adults who used the highest amount of resources in the hospital accounted for 5.7 times higher pharmacy costs than those in the lower resource use categories.

"While the number of adult congenital heart patients who undergo surgery at pediatric hospitals continues to increase, we also found that the lion's share of surgical costs is with pediatric patients," Benavidez said.

The cost for pediatric patients may be higher because they undergo highly complex surgical procedures. "The pediatric patients are resource intensive in their own right given that their extreme complexity requires highly specialized processes to care adequately for these infants and children."

Co-authors are Yuli Y. Kim, MD; Kimberlee Gauvreau, ScD; Emile A. Bacha, MD and Michael J. Landzberg, MD.

CONGENITAL CARDIOLOGY TODAY

Headquarters: 824 Elmcroft Blvd., Rockville, MD 20850 USA

Publishing Management:

- Tony Carlson, Founder & Senior Editor - *TCarlsonmd@gmail.com*
- Richard Koulbanis, Publisher & Editor-in-Chief - *RichardK@CCT.bz*
- John W. Moore, MD, MPH, Medical Editor - *JMoore@RCHSD.org*

Editorial Board:

Teiji Akagi, MD; Zohair Al Halees, MD; Mazeni Alwi, MD; Felix Berger, MD; Fadi Bitar, MD; Jacek Bialkowski, MD; Philipp Bonhoeffer, MD; Mario Carminati, MD; Anthony C. Chang, MD, MBA; John P. Cheatham, MD; Bharat Dalvi, MD, MBBS, DM; Horacio Faella, MD; Yun-Ching Fu, MD; Felipe Heusser, MD; Ziyad M. Hijazi, MD, MPH; Ralf Holzer, MD; Marshall Jacobs, MD; R. Krishna Kumar, MD, DM, MBBS; John Lamberti, MD; Gerald Ross Marx, MD; Tarek S. Momenah, MBBS, DCH; Toshio Nakanishi, MD, PhD; Carlos A. C. Pedra, MD; Daniel Penny, MD, PhD; James C. Perry, MD; P. Syamasundar Rao, MD; Shakeel A. Qureshi, MD; Andrew Redington, MD; Carlos E. Ruiz, MD, PhD; Girish S. Shirali, MD; Horst Sievert, MD; Hideshi Tomita, MD; Gil Wernovsky, MD; Zhuoming Xu, MD, PhD; William C. L. Yip, MD; Carlos Zabal, MD

Statements or opinions expressed in Congenital Cardiology Today reflect the views of the authors and sponsors, and are not necessarily the views of Congenital Cardiology Today.

CCS.12

Congenital Cardiology Solutions

Don't miss the latest in congenital cardiology education happening at ACC's Congenital Cardiology Solutions (CCS.12), which takes place at ACC.12 in Chicago, March 24 – 27, 2012. Explore the latest in science and patient care across the continuum of congenital heart disease, from newborn to adults.

CCS.12 will feature sessions focusing on —

- Quality improvement
- Transition of congenital heart disease patients
- Complex issues in the care of the adult congenital heart disease patient
- Challenging CHD imaging issues
- Debates on medical therapy
- Innovations in congenital care
- Dedicated study session to earn ABP MOC Part 2 credit
- CCS.12 Spotlight session featuring live and taped cases

Plus, don't miss the 2012 Dan G. McNamara Lecture presented by Jane Somerville, MD, FACC. Her lecture, "50 Years with Cardiac Surgeons," will chronicle her medical professional life, including her passion for cardiac surgery and specifically congenital heart disease. She will also discuss relevant advances made from the 1960s through the 21st Century and the need for advancements in adult congenital heart disease.

Register by Feb. 15, 2012 to save!

Go to *www.accscientificsession.org/meeting* for more information!

ACC.12

61st Annual Scientific Session & Expo

ACC-i2 with TCT
innovation in intervention

March 24 – 27, 2012 • CHICAGO
Exhibits: March 24 – 26

SIZING UP THE FUTURE AND TARGETING A BRIGHTER TOMORROW

PTS® SIZING BALLOONS
FOR ACCURATE MEASUREMENT

OF SELECTING THE APPROPRIATELY SIZED OCCLUDER DEVICE

X™ LINE
HOLDING THE LINE

BRAIDED INNER TUBING AND RADIOPAQUE MARKER BANDS FOR MAINTAINING STRENGTH & TRACKABILITY

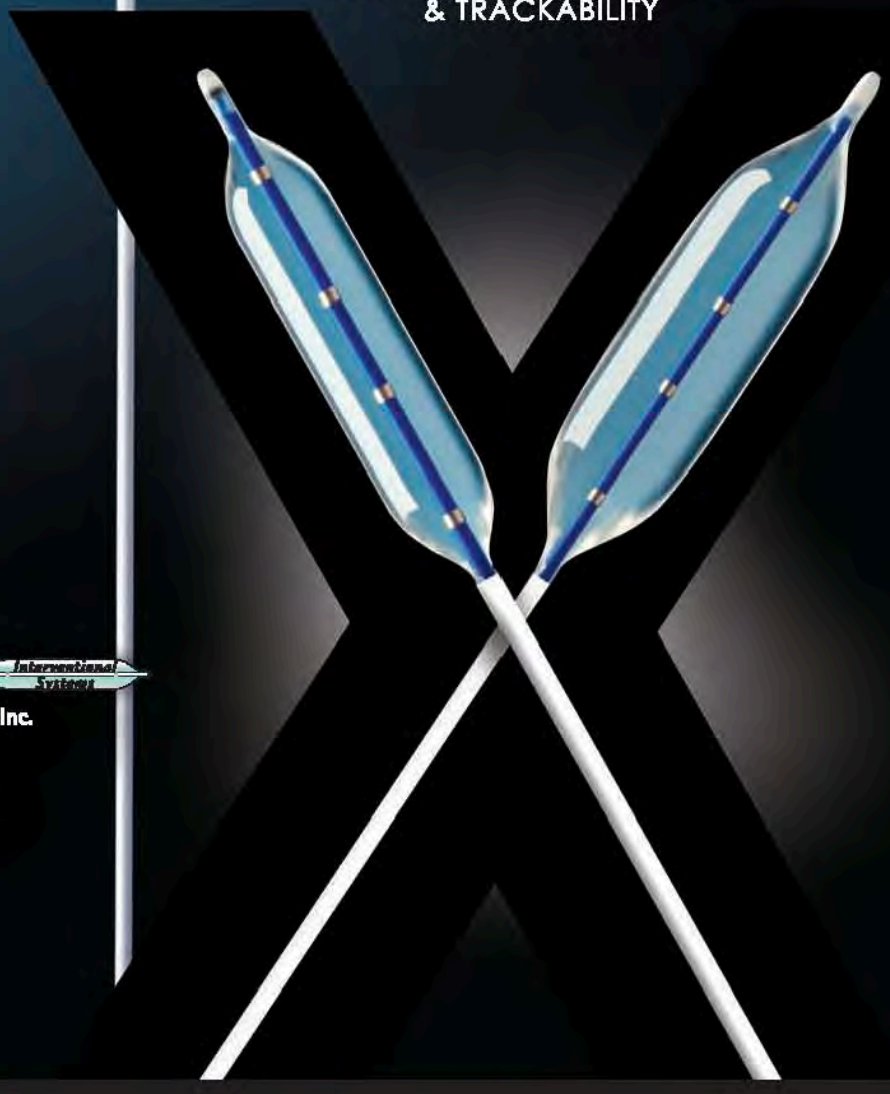

B|BRAUN

B. Braun Interventional Systems Inc.
824 Twelfth Avenue
Bethlehem, PA 18018
Tel: 1-877-VENA CAV (836-2228)
Fax: 610-266-3982

www.bisusa.org